Heterologous expression and characterization of bacterial 2-C-methyl-d-erythritol-4-phosphate pathway in Saccharomyces cerevisiae

Citation: Carlsen, Simon, Parayil Kumaran Ajikumar, Luca Riccardo Formenti, Kang Zhou, Too Heng Phon, Michael Lynge Nielsen, Anna Eliasson Lantz, Morten C. Kielland-Brandt, and Gregory Stephanopoulos. "Heterologous Expression and Characterization of Bacterial 2-C-Methyl-d-Erythritol-4-Phosphate Pathway in Saccharomyces Cerevisiae." Applied Microbiology and Biotechnology 97, no. 13 (May 1, 2013): 5753–5769.

As Published: http://dx.doi.org/10.1007/s00253-013-4877-y

Publisher: Springer-Verlag

Persistent URL: http://hdl.handle.net/1721.1/107177

Version: Author's final manuscript: final author's manuscript post peer review, without publisher's formatting or copy editing

Heterologous expression and characterization of bacterial 2-*C*-methyl-D-erythritol 4-phosphate pathway in *Saccharomyces cerevisiae*

Simon Carlsen*†, Parayil Kumaran Ajikumar†[1], Luca Riccardo Formenti*, Kang Zhou†‡, Too Heng Phon‡, Michael Lynge Nielsen*[,2], Anna Eliasson Lantz*, Morten C. Kielland-Brandt*, Gregory Stephanopoulos†[§]

* Department of Systems Biology, Technical University of Denmark, DK-2800 Kongens Lyngby, Denmark

† Department of Chemical Engineering, Massachusetts Institute of Technology (MIT), Cambridge, MA 02139, USA.

‡ Chemical and Pharmaceutical Engineering Program, Singapore-MIT Alliance, 117546 Singapore.

[1] Present address: Manus Biosynthesis, 790 Memorial Drive, Cambridge, MA 02139, USA.

[2] Present address: Novozymes A/S, Krogshoejvej 36, DK-2880 Bagsvaerd, Denmark.

[§] Corresponding author: Phone: 617.253.4583. Fax: 617.253.3122. Email: gregstep@mit.edu

Abstract

Transfer of a biosynthetic pathway between evolutionary distant organisms can create a metabolic shunt capable of bypassing the native regulation of the host organism, hereby improving the production of secondary metabolite precursor molecules for important natural products. Here, we report the engineering of *Escherichia coli* genes encoding the 2-*C*-methyl-D-erythritol 4-phosphate (MEP)-pathway into the genome of S*accharomyces cerevisiae* and characterization of intermediate metabolites synthesised by the MEP pathway in yeast. Our UPLC-MS analysis of the MEP pathway metabolites from engineered yeast showed that the

pathway is active until the synthesis of 2-*C*-methyl-D-erythritol-2,4-cyclodiphosphate (MEC), but appears to lack functionality of the last two steps of the MEP-pathway, catalyzed by the [4Fe-4S] iron sulfur cluster proteins encoded by *ispG* and *ispH*. In order to functionalize the last two steps of the MEP-pathway we co-expressed the genes for the *E. coli* iron sulfur cluster (ISC)-assembly machinery. By deleting *ERG13*, thereby incapacitating the MVA-pathway, in conjunction with labeling experiments with U-$^{13}C_6$ glucose and growth experiments, we found that the ISC-assembly machinery was unable to functionalize *ispG* and *ispH*. However, we have found that *leuC* and *leuD*, encoding the hetero-dimeric iron-sulfur cluster protein, isopropylmalate isomerase, can complement the *S. cerevisiae leu1* auxotrophy. To our knowledge, this is the first time a bacterial iron-sulfur cluster protein has been functionally expressed in the cytosol of *S. cerevisiae* under aerobic conditions and shows that *S. cerevisiae* has the capability to functionally express at least some bacterial iron-sulfur cluster proteins in its cytosol.

Keywords: *Metabolic engineering, terpenoids, MEP pathway, Heterologous expression, S. cerevisiae, Iron-sulfur cluster proteins*

Introduction

Isoprenoids, comprising more than 55,000 compounds, holds great potential as pharmaceuticals, flavors, fragrances, and in general high-value chemicals (Breitmaier ; McGarvey and Croteau 1995). The complexity of these compounds and their relative scarcity in nature however render their production uneconomical and difficult via chemical synthesis or extraction. Here, metabolic engineering is an enabling technology for engineering heterologous biosynthesis in microorganisms towards developing scalable production methods (Ajikumar et al. 2008; Pirie et al. 2013; Yadav et al. 2012). Such engineering is not straightforward and requires optimization to

establish an efficient biosynthetic pathway for synthesizing the product of interest, avoiding byproduct formation, and improving precursor supply (Keasling 2010). Developments in metabolic engineering over the past two decades have significantly improved our ability to design, construct and optimize biosynthetic pathways in microorganisms (Keasling 2012; Stephanopoulos 2012). Isoprenoid biosynthesis has been engineered in both prokaryotic, *E. coli* and eukaryotic, yeast cells for heterologous production of complex terpeneoid molecules (Ajikumar et al. 2010; Alper et al. 2005; Kroll et al. 2009; Martin et al. 2003; Ro et al. 2006; Wang et al. 2010).

Isoprenoids are biosynthesized from isopentenyl diphosphate (IPP) produced in yeast by the mevalonate (MVA) pathway, starting with acetyl-CoA, and in *E. coli* by the 2-*C*-methyl-D-erythritol 4-phosphate (MEP) pathway, starting with pyruvate and glyceraldehyde-3-phosphate (G3P) (Figure 1) (Ajikumar et al. 2008). The MEP-pathway has been found to be stoichiometrically superior and less byproduct accumulating compared to the MVA-pathway (Dugar and Stephanopoulos 2011). Recently, the *E. coli* MEP pathway was engineered for high level production of terpenoids and the bottleneck inhibitory steps identified (Ajikumar et al. 2010). In other research, Maury and coworkers amplified the seven MEP-pathway genes from *E. coli* genomic DNA and expressed them in *S. cerevisiae* using a dual galactose inducible promoter system based on the *GAL1*-promoter and the *GAL10*-promoter (Maury et al. 2008). To test the activity of the MEP-pathway in *S. cerevisiae,* the native MVA-pathway which supplies precursors for ergosterol and other essential compounds, was inhibited with the hypocholesterolemic drug lovastatin, which specifically inhibits the HMG-CoA reductase (Alberts et al. 1980) and prevents growth of wild type yeast (Maury et al. 2008). Although Maury et al. (2008) reported that the MEP pathway expressing yeast showed some growth in the

presence of lovastatin, significantly lower levels of terpenoids were produced by this strain compared to other native and non-native isoprenoid pathway engineered cells (Ajikumar et al. 2010; Martin et al. 2003; Ro et al. 2006).

In the present study, we sought to engineer the MEP-pathway into *S. cerevisiae*, and characterize metabolites in the pathway to identify bottlenecks. In order to create a stable strain amenable for further genetic modification, we chose to chromosomally integrate the seven MEP-pathway genes from *E. coli* (Table 1) with the addition of the *Idi* gene, which encodes the *E. coli* IPP/dimethylallyl diphosphate (DMAPP) isomerase. These eight genes where synthesized and codon optimized to improve their expression in *S. cerevisiae*. To test whether the chromosomally integrated pathway were functional in *S. cerevisiae*, we deleted the *ERG13* gene, which encodes the HMG-CoA synthase of the MVA-pathway. In contrast to the previous report (Maury et al. 2008), the *E. coli* MEP-pathway chromosomally expressed in *S. cerevisiae* was unable to support growth in the absence of IPP supplied by the MVA-pathway. By analyzing the strain for MEP-pathway metabolites using liquid chromatography – mass spectrometry, we identified both DXP and 2-*C*-methyl-D-erythritol 2,4-cyclodiphosphate (MEC). The results indicate that the MEP pathway is active up to MEC, and that the problem thus originates from insufficient active expression of one or both of the two genes (*ispG* and *ispH*) downstream of MEC. We thereafter searched the literature to elucidate whether *S. cerevisiae* meets the co-factor requirements for the entire MEP-pathway (Table 2). From Table 2.1 it can be seen that all co-factor requirements for the first five pathway steps are fulfilled. However, step 6 and 7 requires ferredoxin or flavodoxin and ferredoxin (flavodoxin) $NADP^+$ reductase to couple the reaction to NADPH for electron transfer. Furthermore, both *ispG* and *ispH* are iron-sulfur cluster proteins which need to be

loaded with a [4Fe-4S]-iron-sulfur cluster (ISC) to be functional (Seemann and Rohmer 2007). Ferredoxin is also an [2Fe-2S] ISC-protein (Blaschkowski et al. 1982).

ISC proteins are ubiquitously found throughout nature, but the approach of assembling these varies from species to species. Three different ISC-assembly pathways have so far been discovered in bacteria, namely the NIF (nitrogen fixation), ISC (iron-sulfur cluster) and SUF (sulfur mobilization) pathway (Tokumoto et al. 2004), whereas a conserved ISC assembly machinery located in the mitochondria is present in eukaryotes. This machinery has been inherited from a bacterial ancestor of the mitochondria and therefore has high similarity to the ISC-assembly machinery found in bacteria (Mühlenhoff and Lill 2000). However, despite localization in the mitochondria, the eukaryotic ISC-assembly machinery must supply ISCs to apo-proteins throughout the cell. This is carried out by the cytosolic iron-sulfur cluster assembly machinery (CIA) (Lill and Mühlenhoff 2008). The CIA machinery is not well characterized, and the exact mechanisms responsible for targeting cytosolic and nuclear apo-proteins to be loaded with ISCs exported from mitochondria are unknown. This obviously complicates engineering of *ispG* and *ispH* to functionalize the gene products within the cytosol of *S. cerevisiae*; in order to remedy this situation we decided to co-express the *E. coli* ISC-assembly machinery with the heterologous MEP-pathway.

The core functions in ISC biogenesis in *E. coli* are encoded by a single gene cluster composed of the following genes: *iscR* – transcriptional regulator, *iscS* – cysteine desulferase (sulfur donor), *iscU* – scaffold, *iscA* – A-type protein, *hscA* – DnaJ-like co-chaperone, *hscB* – DnaK-like chaperone, *fdx* – ferredoxin and *iscX* – unknown function, found to interact with *iscS* (Py and Barras 2010; Tokumoto et al. 2002). In addition to these 8 genes, the *ErpA* gene, encoding another A-type protein, is essential in *E. coli* for converting *ispG* from its apo form to its holo

form (Loiseau et al. 2007). Furthermore, the *E. coli* CyaY gene, encoding frataxin, takes part in ISC-assembly, probably as an iron-donor (Yoon and Cowan 2003). Bedekoviks et al. (2007) showed that a mitochondrially targeted version of the *E. coli CyaY* gene could functionally complement the *yfh1* deletion in *S. cerevisiae* (Bedekovics et al. 2007). *Yfh1 has* previously been found to be important for ISC-biogenesis in yeast, hereby further strengthening the evidence that frataxin is required for ISC-assembly (Duby et al. 2002). Finally, Justino et al. (2007) showed that the *E. coli YtfE*-encoded protein acts as a repair protein to mend ISC-proteins that have been damaged due to nitrosative stress (Justino et al. 2007).

Iron storage and sequestration in a biological system is of outmost importance to ensure that the iron is soluble and thereby accessible where necessitated and to avoid the formation of reactive oxygen species, e.g. through the Haber-Weiss-Fenton reaction, which generates hydroxyl radicals (Aisen et al. 2001). Most organisms use the polymeric protein ferritin to store iron. Even though *S. cerevisiae* contains ferritin, the majority of the iron stored within the cell is located in the vacuole (Raguzzi et al. 1988). Little is known about how iron is transported within the yeast cell, and it is unknown whether the iron stored in the vacuole is available to a heterologous ISC-machinery. It has previously been found that iron storage in *S. cerevisiae,* and therefore tolerance towards stress induced by high extracellular iron concentrations, can be improved by heterologous expression of human hetero-polymeric ferritin (Kim et al. 2003). We therefore decided to additionally express the *E. coli Bfr*, *FtnA*, and *Bfd* genes, encoding the bacterioferritin, ferritin and bacterioferritin-associated ferredoxin, respectively. These iron storage genes together with the ISC-machinery genes, the ISC repair gene and the *Fdx*, *Fpr*, and *FldA* genes, encoding ferredoxin, ferredoxin (flavodoxin) $NADP^+$ reductase, and flavodoxin 1 (Bianchi et al. 1993; Nakamura et al. 1999; Puan et al. 2005), make up the supporting system

that we hypothesized would be required to functionalize the MEP-pathway expressed in *S. cerevisiae*. Here we report the cloning and expression of these 16 genes combined with the 8 MEP-pathway genes (including *Idi*), together with a quantitative analysis of this complex system.

Materials and Methods

Chemicals, enzymes and growth media

Unless otherwise stated, all chemicals were purchased from Sigma-Aldrich®, St. Louis, MO, and all enzymes from New England Biolabs Inc., Ipswich, MA. *E. coli* cells were grown in BD Difco™ LB broth from BD Diagnostic Systems, Sparks, MD. For selection and maintenance of plasmids, ampicillin was added to a final concentration of 100 mg/l. *S. cerevisiae* cultures that required no auxotrophic selection were grown on YPD, composed of: 10 g/l Bacto™ yeast extract, BD Diagnostic Systems; 20 g/l Bacto™ peptone, BD Diagnostic Systems; and 20 g/l dextrose. For auxotrophic selection, *S. cerevisiae* was grown on SC-medium with the appropriate nutrient(s) omitted or SD for prototrophic strains. SC medium was composed of 6.7 g/l Yeast Nitrogen Base (YNB) without amino acids, BD Diagnostic Systems; CSM – amino acid dropout mixture (amount according to manufacturer's recommendation), Sunrise Science Products, Inc., San Diego, CA; and 20 g/l dextrose or galactose. SD was made the same way as SC with the difference of omitting the CSM amino acid dropout mixture. All media components and media besides YNB were sterilized by autoclaving. YNB was sterilized by filtration.

Plasmids and strains

The strains and plasmids acquired for this study can be seen from Table 2. Every cloning for the construction of the plasmids described below was carried out by treating the recipient plasmids with endonuclease(s), purification by gel-electrophoresis and recovery by gel extraction using

the PureLink™ Quick Gel Extraction Kit, Life Technologies, Grand Island, NY, followed by ligation to the insert using T4 DNA ligase. Each insert was either prepared by removing it from the plasmid harboring it by endonuclease digestion followed by gel-electrophoresis and purification in the same way as the recipient plasmid, or amplified by PCR, purified using the QIAquick PCR Purification Kit, Valencia, CA, treated with endonucleases and purified again using the QIAquick PCR Purification Kit. All constructs were verified by sequencing. The DNA ladder used as size reference was the Quick-Load® 1 kb DNA Ladder from New England Biolabs Inc., Ipswich, MA (bands corresponds to the following DNA lengths: 0.5, 1.0, 1.5, 2.0, 3.0, 4.0, 5.0, 6.0, 8.0, 10.0 kb).

Construction of expression cassettes

For expression of the genes of interest, four expression cassettes were created and tested for their ability to mediate transcription by verifying that they could express the yeast enhanced green fluorescent protein (yeGFP). This was done on the basis of the plasmids pRS414TEF and pRS415GPD in which the yeGFP from pKT127 was inserted by *Spe*I/*Xho*I digestion. The pRS414TEF with the insert yeGFP was modified by exchanging the CYC1t with the ADH1t, ACT1t and ENO2t by *Xho*I/*Kpn*I digestion. The TEF1p was substituted with the PGK1p in the plasmid with the ACT1t, and with the TEF2p in the plasmid with the ENO2t, by *Sac*I/*Spe*I digestion. The replacement promoters and terminators were obtained by PCR from CEN.PK 113-7D genomic DNA (gDNA) using the primers containing adaptamers with the respective restriction sites (see Table 3). This resulted in the construction of 4 expression cassettes harboring yeGFP, namely the *TEF1p-yeGFP-ADH1t*, *TDH3p (GPDp)-yeGFP-CYC1t*, *PGK1p-yeGFP-ACT1t* and *TEF2p-yeGFP-ENO2t* in the pSCX001, pSCX002, pSCX003 and pSCX004 plasmids, respectively.

The 8 MEP-pathway genes were purchased codon optimized for *S. cerevisiae* from DNA 2.0, Menlo Park, CA, flanked by *Spe*I (5') and *Xho*I (3') restriction sites. The sequences of the codon optimized genes have been deposited to Genbank, cf. *idi* (accession number: KC571266), *ispH* (accession number: KC571267), *dxr* (accession number: KC571268), *ispG* (accession number: KC571269), *dxs* (accession number: KC571270), *ispE* (accession number: KC571271), *ispD* (accession number: KC571272), *ispF* (accession number: KC571273). Using these restriction sites the genes were cloned into expression cassettes (see Table 4). The 16 ISC-assembly machinery genes were amplified from *E. coli* K12, MG1655 gDNA using Phusion® High-Fidelity DNA Polymerase (applied for all PCR reactions described in section 2) and primers listed in Table 4. The forward and reverse primers were designed with adaptamers containing *Spe*I and *Xho*I restriction sites respectively. These restriction sites were used to clone the genes into their designated expression cassettes. Supplementary Figure S1 shows the graphical overview of the expression cassette construction.

Construction of plasmids for integration of multiple expression cassettes

To integrate the 8 MEP-pathway genes in the genome of *S. cerevisiae*, two plasmids with 4 expression cassettes each were constructed based on the pUC19 plasmid. A 1750 bp fragment containing the *HIS2* ORF with 352 bp upstream of the start codon and 390 bp downstream of the stop codon, and a 1427 bp fragment containing the *ADE1* ORF with 332 bp upstream of the start codon and 274 bp downstream of the stop codon, were amplified from CEN.PK113-7D derived gDNA by PCR with primers containing *Hin*dIII adaptamers (see Table 3) and separately cloned into pUC19 digested with *Hin*dIII. The direction of the insert was determined by sequencing. The *Aat*II sites in the backbone of the constructed vectors and in the *HIS2* ORF were removed by introducing silent point mutations, using the QuikChange® Multi Site-Directed Mutagenesis Kit,

Stratagene, La Jolla, CA. A new multiple cloning site (MCS) comprised of two complementary primers (5'-GCGCGAGCTCCTCGAGGGGCCCAAGCTTGACGTCGTCGACCCTAGGCTGCAGCTTA AGTCTAGAGGTACCGCGC-3', which were annealed and subsequently digested with *Sac*I and *Kpn*I, were inserted into the plasmids treated with *Sac*I and *Kpn*I to create pSC600 (with the *HIS2* marker) and pSC700 (with the *ADE1* marker).

dxs, *ispF*, *ispE*, and *ispD* were treated with *Spe*I and *Xho*I restriction endonucleases and inserted into pSCX001, pSCX003, pSCX002 and pRS414TEF, respectively, hereby creating the following expression cassettes: *TEF1p-dxs-ADH1t*, *PGK1p-ispF-ACT1t*, *TDH3p-ispE-CYC1t*, and *TEF1p-ispD-CYC1t*. *ispG*, *ispH*, *ispC*, and *idi* were treated with *Spe*I and *Xho*I restriction endonucleases and inserted into pRS414TEF, pSCX002, pSCX003, and pSCX001 respectively, hereby creating the following expression cassettes: *TEF1p-ispG-CYC1t*, *TDH3p-ispH-CYC1t*, *PGK1p-ispC-ACT1t*, and *TEF1p-idi-ADH1t*. The cassettes were amplified by PCR with the primers listed in Table 3, purified, and digested with the sets of restriction endonucleases also stated in Table 3. The *dxs*, *ispF*, *ispE*, and *ispD* expression cassettes were in the order listed here sequentially inserted in pSC600 to create pSC604. The *ispG*, *ispH*, *ispC*, and *idi* expression cassettes were in the order listed here sequentially inserted in pSC700 to create pSC704.

For chromosomal integration of the expression cassettes containing the *bfr*, *FtnA*, *bfd* and *YftE* genes, a plasmid based on the pUC19 derived pSC700 plasmid was applied. The genes were amplified from *E. coli* K-12, MG1655 gDNA by PCR with primers listed in Table 4, digested with *Spe*I and *Xho*I and purified. *YtfE* and *FtnA* were inserted into the pSCX002 plasmid treated with *Spe*I and *Xho*I by ligation; and *bfr* and *bfd* in the same way into pSCX001 and pSCX002, respectively. The following expression cassettes were hereby constructed: *TDH3p-YtfE-CYC1t*,

TEF1p-bfr-ADH1t, *PGK1p-bfd-ACT1t*, and *TDH3p-FtnA-CYC1t*. The expression cassettes were amplified by PCR using the primers listed in Table 3, and digested with the sets of restriction endonucleases specified in Table 3. The *YtfE*, *bfr*, *bfd*, and *FtnA* expression cassettes were in the order listed here sequentially inserted into pSC700, whereafter the *ARG4* marker was inserted between the *Hin*dIII and *Bam*HI sites to construct pSC804. The *ARG4* marker was prior to the insertion amplified from CEN.PK113-7D derived gDNA with primers designed to amplify a DNA sequence from 546 bp upstream of the start codon to 364 bp downstream of the stop codon (primers listed in Table 3), digested with *Hin*dIII and *Bam*HI, and purified.

To ensure high expression of the 12 remaining ISC-assembly machinery genes, we created two plasmids with 6 of the expression cassettes each targeting them into the YPRCδ15 and YPRCτ3 loci respectively, since integration of two different *lacZ* expression cassettes into these Ty remnants has given high expression (Flagfeldt et al. 2009). We first separately introduced DNA sequences homologous to the upstream parts of the YPRCδ15 and YPRCτ3 loci into pUC19. The DNA was amplified from F1702 derived gDNA using reverse primers containing adaptamers which introduced the *Avr*II and *Not*I restriction sites. These two sites were used to digest the two plasmids, and the two first expression cassettes were amplified with primers introducing a *Nhe*I restriction site in front of the promoter and an *Avr*II and a *Not*I restriction site following the terminator; since *Avr*II and *Nhe*I are compatible, this allowed the insert treated with *Nhe*I and *Not*I to be inserted into the two plasmids, leaving behind a new set of *Avr*II and *Not*I restriction sites. This approach was iteratively used (see Supplementary Figure S2) to insert the expression cassettes into the two plasmids, finally creating the plasmid pSCFeS107TRP, containing the *iscX*, *iscR*, *iscS*, *fdx*, *TRP1*, *cyaY*, and *iscU* expression cassettes; and pSCFeS207LEU, containing *hscB*, *fpr*, *iscA*, *erpA*, *LEU2*, *hscA* and *fldA*. The last insert in each of the two plasmids was the

DNA sequences homologous to the downstream of the YPRCδ15 and YPRCτ3 loci, respectively. All primers used for the construction of pSCFeS107TRP and pSCFeS207LEU are listed in Table 3. A schematic representation of the construction of the plasmids for integration of multiple expression cassettes is summarized in Supplementary Table S1.

Construction of other plasmids

ERG13 was deleted by a cassette constructed by introducing a 213 bp sequence identical to the gDNA sequence upstream of the *ERG13* start codon between the *Hin*dIII and *Pst*I restriction sites and a 272 bp sequence identical to the gDNA sequence downstream of the *ERG13* stop codon between the SpeI and SacI restriction sites of pUG72, hereby creating plasmid pSCΔ001. The sequences were amplified from F1702 derived gDNA using the primers listed in Table 3.

To test whether *leuC* and *leuD* can complement the *leu1* auxotrophy, three plasmids were constructed, namely pESC-leuC, pESC-leuC/D and pESC-LEU1. pESC-leuC was constructed from pESC-URA by inserting *leuC* between the *Bam*HI and *Hin*dIII restriction sites. pESC-leuC-D was constructed by inserting *leuD* between the *Eco*RI and *Sac*I sites of pESC-leuC. The pESC-LEU1 plasmid was constructed by inserting *LEU1* between the *Bam*HI and *Xho*I restriction sites of pESC-URA. *LeuC* and *leuD* were amplified from *E. coli* gDNA and *LEU1* from F1702 gDNA using the primers listed in Table 3.

All final plasmids constructed in this study are listed in Table 5, and their maps can be seen from Figure S3 in the Supplementary material.

Construction of yeast strains

All transformations of *S. cerevisiae* were carried out using the lithium acetate/polyethylene glycol method according to (Daniel Gietz and Woods 2002). Transformants were selected on SC with the appropriate nutrient(s) omitted. The constructed strains were verified by extraction of

gDNA using the Wizard® Genomic DNA Purification Kit, Promega, Madison, WI, followed by PCR amplification of all the integrated ORFs. Self-replicating plasmids were used directly to transform *S. cerevisiae*, whereas the plasmid destined for genomic integration was linearized. Prior to transformation of *S. cerevisiae* the plasmids pSC604, pSC704 and pSC804 were linearized by digestion with *Msc*I, *Hpa*I and *Age*I endonucleases respectively to facilitate their integration into the non-functional markers present in the yeast genome. The pSCFeS107TRP and pSCFeS207LEU integration cassettes were removed from their respective plasmids by digestion with *Pac*I and *Not*I endonucleases, and the *ERG13* deletion cassette was removed from the pSCΔ001 plasmid by *Not*I and *Sac*II digestion. The order in which the strains were constructed by transformation with the individual plasmids or cassettes can be seen from Table 6.

Test of expression cassette functionality using *yeGFP*

The strains SCX001, SCX002 and SCX004 were grown on SC-TRP and SCX003 on SC-LEU plates at 30 °C until colonies had formed. To test the expression of *yeGFP* the colonies were visually inspected using the Safe Imager™ 2.0 Blue-Light Transilluminator, Life Technologies, Grand Island, NY, with corresponding filter.

Liquid chromatography – Mass spectrometry analysis of MEP-pathway metabolites

SCMEP and SCMEP-FeS2-IS were grown in 5 ml SC-ADE-HIS and SC-ADE-ARG-HIS-LEU-TRP respectively at 30 °C at 250 rpm orbital shaking until the OD_{600} reached 1. Cell suspensions equivalent to 3ml OD600=1 cells were withdrawn at middle exponential growth phase for measuring MEP pathway metabolites. The cell suspension was centrifuged for 1 min, and the cell pellets were resuspended in 1 ml acidic extraction solution (methanol/acetonitrile/ddH_2O 40:40:20, 0.1 M formic acid). The cells were completely lysed by using 200 µl glass beads in

Mini-Beadbeater-16 (Biospec). Following centrifugation, the supernatant was purified through a LC-NH2 resin (Sigma). The resin bound with the metabolites was eluted with 400 µl 1% NH_4OH solution after centrifugation, and pH of eluate was subsequently adjusted to acidic (pH=5) by 3 µl acetic acid (Zhou et al. 2012b). An aqueous solution containing 15 mM acetic acid and 10 mM tributylamine, and methanol were used as mobile phase with a UPLC C18 column (Waters CSH C18 1.7 µm 2.1x 50 mm) as follows. The elution was done at 0.15 ml/min with gradient (start: 0% methanol, 1.8 mins: 0% methanol, 3.1 mins: 40% methanol, 4.9 mins: 40% methanol, 5.4 mins; 90% methanol, 9.5 mins: 90% methanol, 10 mins: 0% methanol). Electrospray ionization was used and mass spectrometry was operated to scan 50-800 m/z in negative mode with -500V end plate voltage and 4500V capillary voltage. Nebulizer gas was provided in 1 bar, drying gas rate was 9 ml/min, and dry gas temperature was 200 °C. Sample injection volume was 5 µL. Retention time is 5.6min and 6.6min for DXP (m/z=213.0170) and MEC (m/z=276.9884), respectively. The peak area was integrated for each metabolite with the software provided by the manufacturer.

Analysis of pathway functionality using U-$^{13}C_6$ glucose

Strain SCMEP-FeS2-IS-ΔERG13 was inoculated at OD_{600} = 0.05 in 5 ml SD medium made with U-$^{13}C_6$ glucose, Cambridge Isotope Laboratories, Andover, MA and grown aerobically for 2 days at 30 °C with 250 rpm orbital shaking. The cells were spun down at 3,000 rpm for 10 min, re-suspended in 2 ml 20% w/v sodium hydroxide in 50% ethanol, transferred to an 8 ml glass tube, and extracted according to Madsen et al. (Madsen et al. 2011). The extract was dried, re-dissolved in 50 µl pyridine, derivatized by addition of 50 µl *N,O*-bis(trimethylsilyl) trifluoroacetamide (BSTFA) + 1 % trimethylchlorosilane (TMCS) according to Nielsen and Madsen (Nielsen and Madsen 2000), and analyzed using GC-MS. A 1-µl sample was analyzed

using splitless injection on a DB-35ms, 30 m, 0.25 mm, 0.25 µm column, Agilent Technologies, Santa Clara, CA, with helium as carrier gas. The temperature of the oven was initially held at 160 °C for 30 sec, then increased to 320 °C at 10 °C/min, and finally held at 320 °C for 3 min. Ergosterol and squalene standards were subjected to the same procedure for authentication.

Verification of gene expression by reverse transcriptase polymerase chain reaction (RT-PCR)

S. cerevisiae cultures (5 mL) were grown at 30 °C until OD_{600} = 1, whereafter the cells were harvested by centrifugation at 3000 g for 10 min and washed with TE-buffer. They were transferred to a 2-ml FastPrep® tube, MP Biomedicals LLC, Solon, OH, and re-suspended in 500 µl TE-buffer. Two hundred µl acid washed glass beads (425-600 µm), Sigma-Aldrich® and 500 µl acidic phenol-chloroform-isoamyl alcohol (125:24:1), pH 4.5, Life Technologies, Grand Island, NY, were added. The cells were disrupted using a Savant FastPrep® FP120 Cell Disrupter, MP Biomedicals LLC. The phases were separated by centrifugation at 18,000 g for 10 min, and 450 ml of the aqueous phase were transferred to a micro-centrifuge tube. Total RNA was precipitated by addition of 3 M sodium acetate (45 µl), pH 5.2 and isopropanol (450 µl), rinsed twice with 80 % ethanol (500 µl) and re-dissolved in nuclease-free water (90 µl), Qiagen, Valencia, CA. The RNA was treated with DNase I, extracted with acidic phenol-chloroform-isoamyl alcohol (125:24:1, 400 µl) pH 4.5 and TE-buffer pH 8.0 (400 µl), then precipitated by sodium acetate and isopropanol and finally re-dissolved in nuclease free water (100 µl). This RNA served as template for RT-PCR using the Illustra™, Ready-To-Go™, RT-PCR Beads from GE Healthcare Biosciences, Pittsburgh, PA. The RNA solution was checked for DNA contamination by PCR using the Taq DNA polymerase. The PCR products were visualized by

gel electrophoresis (0.75 % agarose in TAE) and staining by Sybr® Safe, Life Technologies, Grand Island, NY.

Evolution of *S. cerevisiae* by serial sub-culturing

Strain SCMEP-FeS2-IS-ΔERG13 was inoculated from glycerol stock in SC-ADE-ARG-HIS-LEU-TRP-URA medium (5 ml) supplemented with mevalonolactone (10 g/l). The strain was incubated at 30 °C for 5 days with 250 rpm orbital shaking. Hereafter the OD_{600} was measured, and re-inoculated into SC-ADE-ARG-HIS-LEU-TRP-URA (5 ml) with mevalonolactone (5 g/l) at OD_{600} = 0.1. This periodical re-inoculation was continued, reducing the mevalonolactone concentration with every re-inoculation. The mevalonolactone was prepared as a stock-solution (500 g/l) according to Dimster-Denk et al. (Dimster-Denk et al. 1994) by dissolving it in dH_2O at 65 °C for 1 h followed by filter sterilization.

Microscopy

The morphology of cells from the serial sub-culturing was investigated using a Nikon Eclipse TE200-S microscope, Nikon Instruments Inc. Melville, NY. The bright field images were obtained at 1000× magnification.

Functional complementation of *leu1* auxotrophy

Strains SC-pESC, SC-leuC, SC-leuC-D and SC-LEU1 were streaked out on SC (galactose)-LEU-URA plates from glycerol stock and incubated at 30 °C for 4 days, and the growth was assessed and documented by photography of the plates.

Results

In order to develop a compatible expression system for multiple genes expression, initially we constructed 4 plasmids based on the pRS-series of *S. cerevisiae*/*E. coli* shuttle plasmids (Mumberg et al. 1995). Each plasmid containing an expression cassette harboring the gene encoding yeGFP was transformed into *S. cerevisiae* F1702, and their ability to mediate expression was verified by visual inspection of the resulting colonies (data not shown). The 4 expression cassettes then served as starting point for creating 24 individual expression cassettes harboring the genes listed in Table 4. After systematic assembly of the 24 expression cassettes into 5 plasmids designed for chromosomal integration, the plasmids were one by one integrated into the genome of F1702. The first two plasmids to be integrated were pSC604 and pSC704, harboring the codon optimized genes encoding the MEP-pathway enzymes to construct the strain designated SCMEP. gDNA from SCMEP was isolated and used as template for PCR reactions confirming that all the genes were indeed integrated (result not shown). To test whether the heterologous MEP-pathway could supply the IPP required to sustain growth, we tried to delete the *ERG13* gene using a deletion cassette. We were unable to obtain viable colonies from which the *ERG13* gene had been knocked out. Several false positive colonies were obtained, probably due to integration of the deletion cassette at a non-specific locus.

The SCMEP strain was then subjected to analysis using UPLC-MS, by which we detected 3.2 ± 0.29 mg DXP per g dry cell weight (DCW) and 5.0 ± 1.8 mg MEC per g DCW (the number following the ± is the standard error of the mean). These results prove that the MEP-pathway is active until MEC, but whether the last two steps are active is impossible to determine based on these results since no HMBPP (detection limit = 0.2 mg/l) could be detected, and it is impossible

to discriminate between the IPP originating from the MVA-pathway and the MEP-pathway. This indicated that the MEP-pathway is insufficient at supplying precursors in quantities that can support growth. However, this is the first time that DXP and MEC have been produced and detected in a *S. cerevisiae* strain.

The last two steps of the MEP-pathway are catalyzed by ISC-proteins, which require an elaborate support machinery to load the apo-proteins with ISC and couple these to NAD(P)H cofactor metabolism for supplying reducing equivalents. To alleviate this potential problem we delineated the proteins that we, based on the literature, hypothesized could be sufficient to decouple the ISC assembly system from *E. coli* and graft it into the cytosol of *S. cerevisiae*. The 16 genes encoding these proteins were by the plasmids pSCFeS107TRP, pSCFeS207LEU and pSC804 integrated into the genome of SCMEP to construct SCMEP-FeS2-IS. gDNA was isolated from SCMEP-FeS2-IS, and all 24 genes were verified by PCR to be inserted within its genome. The results of the PCR can be seen from Figure 2A.

After verifying that all the genes had been inserted into the chromosome, we once more tried to delete the *ERG13* gene, but no viable colonies were obtained. This result does as aforementioned not prove that the MEP-pathway is inactive but only that the activity is too low to support growth, so we once again tested the strain using LC-MS, but have not observed any significant change in MEC compared to the SCMEP strain. However the DXP concentration had increased to 7.9 ± 1.4 mg/g DCW; currently the reason for increased accumulation of DXP is unkown. To be able to delete *ERG13* we had to supplement the medium with 10 g/L mevalonolactone, which serves as a source for mevalonate. Thirty colonies were screened by extraction of gDNA followed by PCR. Three colonies (colony 13, 25 and 29) were identified by PCR to have the deletion cassette integrated in the correct locus and no duplication of *ERG13* prior to the deletion

(Figure 2B). These strains were named SCMEP-FeS-IS-ΔERG13-strain13, SCMEP-FeS-IS-ΔERG13-strain25 and SCMEP-FeS-IS-ΔERG13-strain29.

In order to find out if the MEP-pathway is active in the SCMEP-FeS2-IS-ΔERG13 strains isolated, they were grown on SD-medium made with uniformly ^{13}C-labelled glucose and unlabeled mevalonolactone as carbon sources. Since *ERG13* was deleted, the only way labeled carbon can end up in IPP is if the MEP-pathway is active. IPP is the first isoprenoid precursor of ergosterol, which is made from 2 FPP units (equivalent to 6 IPP units) forming squalene, which then undergoes several modifications to form ergosterol. During these modifications, 3 carbon atoms are lost due to the C14-demethylase and C4-decarboxylase activities encoded by *ERG11* and *ERG26*, respectively. Furthermore, a carbon is gained through the activity of the C24-methyl transferase, encoded by *ERG6* (Veen and Lang 2004). If the MEP-pathway is active one would expect to see a shift in the molecular weight of ergosterol of 3 Daltons or higher, whereas a shift of 1 Dalton just indicates the labeled carbon gained from the C-24 methyl transferase. The ergosterol extracts from the 3 strains grown on medium with either uniformly ^{13}C-labelled glucose or regular glucose were analyzed on GC-MS and the peaks corresponding to squalene and ergosterol identified by comparisons of squalene and ergosterol standards. An example of the results obtained from this analysis can be seen from Supplementary Figure S4. The peak for the molecular weight of un-fragmented ergosterol derivatized with BSTFA is located at approximately 468 Daltons (corresponding to the M0 peak), and its eight mass-isotopomers peaks M1, M2, M3, M4, M5, M6, M7 and M8 (corresponding to M0 + increments of 1 Dalton respectively) were integrated for ergosterol isolated from the SCMEP-FeS2-IS-ΔERG13 strain grown on either uniformly C^{13}-labelled glucose or regular glucose in triplicate. The results from all the strains were almost identical. The result from SCMEP-FeS-IS-ΔERG13-strain13 can be

seen from Figure 3. The species that are heavier than M0 and M1 for the unlabeled and labeled, respectively, are due to natural occurrence of C^{13}.These results show a shift of 1 Dalton from the unlabeled to the labeled, which indicates that the MEP-pathway has a very limited flux if any at all.

To test if all 24 genes were expressed, total RNA was isolated from SCMEP-FeS2-IS and tested for residual DNA by PCR. No DNA was found (results not shown). The RNA was used as template in RT-PCR reactions with primers pairs (Table 4) designed to amplify the entire ORF of the individual genes. The result of the RT-PCR reactions (Figure 4) showed that, except for *bfd*, *fldA* and *hscA*, all the genes are expressed. The experiment was therefore repeated, and *bfd* and *fldA* were also shown to be expressed (data not shown). However, it was not possible to detect any band for *hscA*. Since the same 4 promoters were used to express the genes, and as all other genes expressed by the same promoter as *hscA*, were expressed, the failure to detect transcription could be due to low mRNA stability, either *in vivo* or post cell breakage. However, lack of *hscA* expression is presumably not detrimental for functionality of the ISC-assembly machinery, since it has been found *in vitro* to be stimulatory rather than absolutely required for the transfer of ISC from the assembly machinery to the apo-proteins (Mansy et al. 2002).

To investigate the possibility that the SCMEP-FeS2-IS-ΔERG13 strains have a finite, albeit low, flux through the MEP-pathway that could be increased, we set out to adapt the cultures to grow with IPP being solely supplied by the MEP-pathway by serial sub-culturing with decreasing amounts of mevalonolactone. Adaptive evolution has previously been found efficient for growth of engineered *S. cerevisiae* strains on xylose (Zhou et al. 2012a). The result of the evolution is summarized in Figure 5. The newly created SCMEP-FeS2-IS-ΔERG13 strains needed 5 g/l mevalonolactone to grow (results not shown), which corresponds with the value reported by

(Umebayashi and Nakano 2003). However, serial sub-culturing for more than a half year resulted in two of the strains being able to grow to a similar OD_{600} in medium with 5 mg/L mevalonolactone, i.e. 1000-fold less. Despite this strong adaptation no mevalonate independent cells could be isolated. In other words, the heterologous MEP-pathway was still unable to support growth. This suggests that the MEP-pathway is inactive, since one would expect it to be possible to evolve a pathway directly linked to growth with low activity to higher activity, whereas evolving a pathway with no activity to become active is less likely. During the directed evolution the morphology of the cells was observed using light microscopy. Figure 6 shows the morphology of the three SCMEP-FeS2-IS-ΔERG13 strains grown in SC-ADE-ARG-HIS-LEU-TRP-URA + 0.25 g/l mevalonolactone. It can be seen that strains 25 and 29 exhibit abnormal morphology, probably due to the stress of low mevalonate availability.

In order to test whether *S. cerevisiae* can functionally express other heterologous [4Fe-4S] ISC-proteins from *E. coli* within its cytosol we decided to test if the *S. cerevisiae* strain JAY20, auxotrophic for leucine due to a deletion of the *LEU1* gene, encoding the second step in the biosynthesis of leucine, catalyzed by the isopropylmalate isomerase, could be complemented by the *E. coli* heterodimeric isopropylmalate isomerase, encoded by *leuC* and *leuD* (Skala et al. 1991). The *leuC* gene was inserted in the pESC-URA plasmid followed by *leuD*, hereby constructing plasmids pESC-leuC and pESC-leuC-D, respectively. As a positive control, *LEU1* from F1702 was inserted in pESC-URA as well. These 3 plasmids together with the pESC-URA plasmid, which served as negative control, were used to transform JAY20. Expression of the genes integrated in pESC-URA was under control of the *GAL1/GAL10* inducible promoter system. The four strains were plated on SC-LEU-URA with galactose as carbon source. The result can be seen from Figure 7 and shows that pESC-leuC-D can complement the *LEU1*

auxotrophy. *leuC* and *leuD* do however have a high degree of homology with *LEU1*, which could explain why they can be loaded with ISC. The mechanism of targeting apo-ISC-proteins to be loaded with ISC and hereby converted to their active holo-form has not yet been elucidated, but this result demonstrates that bacterial ISC-proteins heterologously expressed in *S. cerevisiae* can be converted to their functional holo-form.

The finding that *S. cerevisiae* is capable of loading cytosolic heterodimeric isopropylmalate isomerase encoded by *leuC* and *leuD* with ISCs does not imply that all bacterial ISC-proteins heterologously expressed within the yeast cytosol can be loaded with ISCs. *ispG* and *ispH* are not the only two ISC-proteins among the proteins required for MEP-functionality. Ferredoxin is also an [2Fe-2S] ISC-protein (Ta and Vickery 1992), and it is involved in the transfer of electrons to *ispG* and *ispH*, as well as electron transfer to ISC-biogenesis. To be functional, ferredoxin therefore needs to be loaded with an ISC, which has to originate from the yeast CIA-machinery, since it cannot originate from the heterologous ISC-assembly machinery; this is because no ISC can be generated through the heterologous expressed ISC-assembly machinery before ferredoxin is converted to its active holo-form. With ferredoxin as a pivotal point for MEP-pathway functionality, emphasis on research to assess whether this protein can be converted to its holo-form is required. If ferredoxin is found only in its apo-form, research should focus on adapting it to be loaded with ISC via the CIA-machinery, since this will be key to functionally express the MEP-pathway in the cytosol of *S. cerevisiae*.

Discussion

S. cerevisiae have several advantageous characteristics making it an ideal host for microbial production of isoprenoids such as well-established large scale fermentation, enabling easy scale-up, GRAS classification by the FDA, which eases the approval of novel products,

compartmentalization for co-localization of enzymes, and strains pre-engineered to express cytochrome P450 species that are important for the downstream decoration of the isoprenoid backbones have been demonstrated (Huang et al. 2008; Truan et al. 1993). The combination of *S. cerevisiae* with the stoichiometrical superior MEP-pathway holds great potential for bypassing native regulation, hereby constructing an excellent platform for isoprenoid production. Our results, MEP-pathway is active until MEC and ISC-proteins can be expressed in the cytosol of yeast, are encouraging for the further quest for functionalizing the MEP-pathway in its entirety(Partow et al. 2012).

The requirements for an elaborate ISC-assembly machinery for *ispG* and *ispH* function, combined with the finding that MEC can be detected in a cell extract, suggest that the MEP-pathway is only active until MEC. This is further supported by the lack of labeled carbon ending up in ergosterol through the MEP pathway, as well as the mevalonolactone requirement of the *erg13Δ* strains. This view contradicts the view expressed by Maury et al. (2008), who used lovastatin in an attempt to find out if the MEP-pathway was active. However, the growth in the presence of lovastatin could have been caused by other circumstances, e.g., a mutation conferring resistance towards the drug. To circumvent the use of lovastatin, Maury et al. [2008] furthermore suggested deleting a gene encoding one of the early steps of the MVA-pathway such as *ERG10*, *ERG13* or *HMG1* and *HMG2*. We deleted *ERG13* in strain SCMEP, which only expresses the MEP-pathway genes, as well as in the SCMEP-FeS2-IS, expressing the MEP-pathway together with all the support genes hypothesized to be required. In neither case were we able to obtain transformants that had lost *ERG13* and could grow without mevalonolactone supplementation. Furthermore previous research did not express any additional genes for coupling the *ispG* and *ispH* to NAD(P)H such as ferredoxin, flavodoxin and ferredoxin

(flavodoxin) oxidoreductase (Maury et al. 2008). *S. cerevisiae* natively possesses ferredoxin, but it is located within the mitochondria and found to be required for the assembly of ISC-proteins (Lange et al. 2000). No evidence of ferredoxin present in the cytosol of *S. cerevisiae* has been reported, and it is therefore probably not available for *ispG* and *ispH*. This is an additional reason to doubt that the MEP-pathway was functional in the *S. cerevisiae* system presented by Maury et al. [2008].

Further research into the requirements for targeting heterologous ISC-apo-proteins to be converted to their holo-form through the CIA machinery could help functionalize the MEP-pathway, whereas the approach of expressing the heterologous ISC-machinery in *S. cerevisiae* could not only help functionalize the MEP-pathway but also help us understand which parts of the *E. coli* ISC-machinery are essential and how this system should be delineated. Alone from *E. coli*, 100 ISC-proteins have been isolated (Fontecave 2006), and being able to functionally express this group of ubiquitous proteins in *S. cerevisiae* encompasses great prospects for biosynthetic production of novel compounds, as well as obtaining a greater understanding of the complex processes involved in ISC-assembly. A *S. cerevisiae* strain pre-engineered to express the machinery required for cytosolic expression of heterologous ISC-proteins would therefore be a great tool in many areas within biotechnological and pharmaceutical research. Our work has showed the initial steps towards obtaining such strains and highlighted the obstacles on the way towards reaching this goal. This will hopefully spark further interest within the area of heterologous expression of ISC-proteins.

Acknowledgements

The authors would like to thank Dr. Hang Zhou, Dr. Jose Avalos and Dr. Gerald R. Fink for contributing the plasmids and yeast strains used in this study and Dr. Christopher Pirie, Manus Biosynthesis, for critical reading of the manuscript. S.C., P.K.A. and G.S. acknowledge the support by the National Institutes of Health, Grant number 1-R01-GM085323-01A1. S.C., L.R.F., M.L.N., A.E.L., M.C.K.B. gratefully acknowledge the funding from the Technical University of Denmark. K.Z. and T.H.P. acknowledge the support from Singapore-MIT Alliance (SMA-2). S.C. and P.K.A. designed the experiments, performed the engineering. SC performed characterization and screening of the strains. K.Z. and T.H.P. carried out the UPLC-MS measurements. S.C., P.K.A., L.R.F., M.L.N., A.E.L., M.C.K.B. and G.S. analyzed the data and wrote the manuscript. All of the authors contributed to discussion of the research. All authors edited and commented on the manuscript.

References

Aisen P, Enns C, Wessling-Resnick M (2001) Chemistry and biology of eukaryotic iron metabolism. Int J Biochem Cell Biol 33(10):940

Ajikumar PK, Tyo K, Carlsen S, Mucha O, Too HP, Stephanopoulos G (2008) Terpenoids: opportunities for biosynthesis of natural product drugs using engineered microorganisms. Mol Pharm 5(2):167-190

Ajikumar PK, Xiao WH, Tyo KEJ, Wang Y, Simeon F, Leonard E, Mucha O, Too HP, Pfeifer B, Stephanopoulos G (2010) Isoprenoid pathway optimization for Taxol precursor overproduction in *Escherichia coli*. Science 330(6000):70-74

Alberts A, Chen J, Kuron G, Hunt V, Huff J, Hoffman C, Rothrock J, Lopez M, Joshua H, Harris E (1980) Mevinolin: a highly potent competitive inhibitor of hydroxymethylglutaryl-coenzyme A reductase and a cholesterol-lowering agent. Proc Natl Acad Sci U S A 77(7):3957-3961

Alper H, Miyaoku K, Stephanopoulos G (2005) Construction of lycopene-overproducing *E. coli* strains by combining systematic and combinatorial gene knockout targets. Nature biotechnology 23(5):612-616

Bedekovics T, Gajdos GB, Kispal G, Isaya G (2007) Partial conservation of functions between eukaryotic frataxin and the *Escherichia coli* frataxin homolog CyaY. FEMS Yeast Res 7(8):1276-1284

Bianchi V, Reichard P, Eliasson R, Pontis E, Krook M, Jörnvall H, Haggård-Ljungquist E (1993) *Escherichia coli* ferredoxin NADP+ reductase: activation of *E. coli* anaerobic ribonucleotide reduction, cloning of the gene (fpr), and overexpression of the protein. J Bacteriol 175(6):1590-1595

Blaschkowski HP, Knappe J, Ludwigfestl M, Neuer G (1982) Routes of flavodoxin and ferredoxin reduction in *Escherichia coli*. Eur J Biochem 123(3):563-569

Breitmaier E Terpenes flavors, fragrances, pharmaca, pheromones. 2006. Wiley-VCH Verlag GmbH & Co. KgaA, Weinheim

Daniel Gietz R, Woods RA (2002) Transformation of yeast by lithium acetate/single-stranded carrier DNA/polyethylene glycol method. Methods Enzymol 350:87-96

Dimster-Denk D, Thorsness MK, Rine J (1994) Feedback regulation of 3-hydroxy-3-methylglutaryl coenzyme A reductase in *Saccharomyces cerevisiae*. Mol Biol Cell 5(6):655

Duby G, Foury F, Ramazzotti A, Herrmann J, Lutz T (2002) A non-essential function for yeast frataxin in iron–sulfur cluster assembly. Hum Mol Genet 11(21):2635-2643

Dugar D, Stephanopoulos G (2011) Relative potential of biosynthetic pathways for biofuels and bio-based products. Nat Biotechnol 29(12):1074-1078

Flagfeldt BD, Siewers V, Huang L, Nielsen J (2009) Characterization of chromosomal integration sites for heterologous gene expression in *Saccharomyces cerevisiae*. Yeast 26(10):545-551

Fontecave M (2006) Iron-sulfur clusters: ever-expanding roles. Nat Chem Biol 2(4):171-174

Huang B, Guo J, Yi B, Yu X, Sun L, Chen W (2008) Heterologous production of secondary metabolites as pharmaceuticals in *Saccharomyces cerevisiae*. Biotechnol Lett 30(7):1121-1137

Justino MC, Almeida CC, Teixeira M, Saraiva LM (2007) *Escherichia coli* di-iron YtfE protein is necessary for the repair of stress-damaged iron-sulfur clusters. J Biol Chem 282(14):10352-10359

Keasling JD (2010) Manufacturing molecules through metabolic engineering. Science 330(6009):1355-1358

Keasling JD (2012) Synthetic biology and the development of tools for metabolic engineering. Metab Eng 14(3):189-95 doi:10.1016/j.ymben.2012.01.004

Kim HJ, Kim HM, Kim JH, Ryu KS, Park SM, Jahng KY, Yang MS, Kim DH (2003) Expression of heteropolymeric ferritin improves iron storage in *Saccharomyces cerevisiae*. Appl Environ Microbiol 69(4):1999-2005

Kroll J, Steinle A, Reichelt R, Ewering C, Steinbüchel A (2009) Establishment of a novel anabolism-based addiction system with an artificially introduced mevalonate pathway: complete stabilization of plasmids as universal application in white biotechnology. Metabolic engineering 11(3):168-177

Lange H, Kaut A, Kispal G, Lill R (2000) A mitochondrial ferredoxin is essential for biogenesis of cellular iron-sulfur proteins. Proc Natl Acad Sci U S A 97(3):1050-1055

Lill R, Mühlenhoff U (2008) Maturation of iron-sulfur proteins in eukaryotes: mechanisms, connected processes, and diseases. Annu Rev Biochem 77:669-700

Loiseau L, Gerez C, Bekker M, Ollagnier-de Choudens S, Py B, Sanakis Y, Teixeira de Mattos J, Fontecave M, Barras F (2007) ErpA, an iron–sulfur (Fe–S) protein of the A-type essential for respiratory metabolism in *Escherichia coli*. Proc Natl Acad Sci U S A 104(34):13626-13631

Madsen KM, Udatha GD, Semba S, Otero JM, Koetter P, Nielsen J, Ebizuka Y, Kushiro T, Panagiotou G (2011) Linking genotype and phenotype of *Saccharomyces cerevisiae* strains reveals metabolic engineering targets and leads to triterpene hyper-producers. PloS one 6(3):e14763

Mansy SS, Wu G, Surerus KK, Cowan JA (2002) Iron-sulfur cluster biosynthesis. J Biol Chem 277(24):21397-21404

Martin VJJ, Pitera DJ, Withers ST, Newman JD, Keasling JD (2003) Engineering a mevalonate pathway in *Escherichia coli* for production of terpenoids. Nat Biotechnol 21(7):796-802

Maury J, Asadollahi MA, Møller K, Schalk M, Clark A, Formenti LR, Nielsen J (2008) Reconstruction of a bacterial isoprenoid biosynthetic pathway in *Saccharomyces cerevisiae*. FEBS Lett 582(29):4032-4038

McGarvey DJ, Croteau R (1995) Terpenoid metabolism. Plant Cell 7(7):1015

Mühlenhoff U, Lill R (2000) Biogenesis of iron-sulfur proteins in eukaryotes: a novel task of mitochondria that is inherited from bacteria. Biochim Biophys Acta 1459(2-3):370

Mumberg D, Muller R, Funk M (1995) Yeast vectors for the controlled expression of heterologous proteins in different genetic backgrounds. Gene 156(1):119-122

Nakamura M, Saeki K, Takahashi Y (1999) Hyperproduction of recombinant ferredoxins in *Escherichia coli* by coexpression of the ORF1-ORF2-iscS-iscU-iscA-hscB-hscA-fdx-ORF3 gene cluster. J Biol Chem 126(1):10-18

Nielsen KF, Madsen JØ (2000) Determination of ergosterol on mouldy building materials using isotope dilution and gas chromatography–tandem mass spectrometry. Journal of Chromatography A 898(2):227-234

Partow S, Siewers V, Daviet L, Schalk M, Nielsen J (2012) Reconstruction and Evaluation of the Synthetic Bacterial MEP Pathway in *Saccharomyces cerevisiae*. PloS one 7(12):e52498

Pirie CM, De Mey M, Prather KLJ, Ajikumar PK (2013) Integrating the protein and metabolic engineering toolkits for next-generation chemical biosynthesis. ACS chemical biology 10.1021/cb300634b

Puan KJ, Wang H, Dairi T, Kuzuyama T, Morita CT (2005) fldA is an essential gene required in the 2-C-methyl-D-erythritol 4-phosphate pathway for isoprenoid biosynthesis. FEBS Lett 579(17):3802-3806

Py B, Barras F (2010) Building Fe–S proteins: bacterial strategies. Nat Rev Microbiol 8(6):436-446

Raguzzi F, Lesuisse E, Crichton RR (1988) Iron storage in *Saccharomyces cerevisiae*. FEBS Lett 231(1):253-258

Ro DK, Paradise EM, Ouellet M, Fisher KJ, Newman KL, Ndungu JM, Ho KA, Eachus RA, Ham TS, Kirby J (2006) Production of the antimalarial drug precursor artemisinic acid in engineered yeast. Nature 440(7086):940-943

Seemann M, Rohmer M (2007) Isoprenoid biosynthesis via the methylerythritol phosphate pathway: GcpE and LytB, two novel iron–sulphur proteins. Comptes Rendus Chimie 10(8):748-755

Skala J, Capieaux E, Balzi E, Chen W, Goffeau A (1991) VII. Yeast sequencing reports. Complete sequence of the *Saccharomyces cerevisiae* LEU1 gene encoding isopropylmalate isomerase. Yeast 7(3):281-285

Stephanopoulos G (2012) Synthetic Biology and Metabolic Engineering. ACS Synthetic Biology

Ta DT, Vickery L (1992) Cloning, sequencing, and overexpression of a [2Fe-2S] ferredoxin gene from *Escherichia coli*. J Biol Chem 267(16):11120-11125

Tokumoto U, Kitamura S, Fukuyama K, Takahashi Y (2004) Interchangeability and distinct properties of bacterial Fe-S cluster assembly systems: functional replacement of the isc and suf operons in *Escherichia coli* with the nifSU-like operon from Helicobacter pylori. J Biol Chem 136(2):199-209

Tokumoto U, Nomura S, Minami Y, Mihara H, Kato S, Kurihara T, Esaki N, Kanazawa H, Matsubara H, Takahashi Y (2002) Network of Protein-Protein Interactions among Iron-Sulfur Cluster Assembly Proteins in *Escherichia coli*. J Biol Chem 131(5):713-719

Truan G, Cullin C, Reisdorf P, Urban P, Pompon D (1993) Enhanced in vivo monooxygenase activities of mammalian P450s in engineered yeast cells producing high levels of NADPH-P450 reductase and human cytochrome b. Gene 125(1):49-55

Umebayashi K, Nakano A (2003) Ergosterol is required for targeting of tryptophan permease to the yeast plasma membrane. J Cell Biol 161(6):1117-1131

Veen M, Lang C (2004) Production of lipid compounds in the yeast *Saccharomyces cerevisiae*. Appl Microbiol Biotechnol 63(6):635-646

Wang C, Yoon SH, Shah AA, Chung YR, Kim JY, Choi ES, Keasling JD, Kim SW (2010) Farnesol production from *Escherichia coli* by harnessing the exogenous mevalonate pathway. Biotechnology and bioengineering 107(3):421-429

Yadav VG, De Mey M, Lim CG, Ajikumar PK, Stephanopoulos G (2012) The future of metabolic engineering and synthetic biology: towards a systematic practice. Metab Eng 14(3):233-41

Yoon T, Cowan J (2003) Iron-sulfur cluster biosynthesis. Characterization of frataxin as an iron donor for assembly of [2Fe-2S] clusters in ISU-type proteins. J Am Chem Soc 125(20):6078-6084

Zhou H, Cheng JS, Wang BL, Fink GR, Stephanopoulos G (2012a) Xylose isomerase overexpression along with engineering of the pentose phosphate pathway and evolutionary engineering enable rapid xylose utilization and ethanol production by *Saccharomyces cerevisiae*. Metab Eng 14(6):611-22 doi:10.1016/j.ymben.2012.07.011

Zhou K, Zou R, Stephanopoulos G, Too HP (2012b) Metabolite Profiling Identified Methylerythritol Cyclodiphosphate Efflux as a Limiting Step in Microbial Isoprenoid Production. PloS one 7(11):e47513

Table 1: MEP-pathway reactions and cofactors

Protein name/ gene name(s)	Substrate(s)/product(s)	Cofactor(s)	Reference	EcoCyc accession number
Dxs/ *dxs*	pyruvate + D-glyceraldehyde-3-phosphate + H^+/ CO_2 + 1-deoxy-D-xylulose 5-phosphate	Thiamine diphosphate; Mg^{2+}; Mn^{2+}	Xiang et al., 2007	G6237
Dxr/ *dxr*	1-deoxy-D-xylulose 5-phosphate + NADPH + H^+/ 2-*C*-methyl-D-erythritol-4-phosphate + $NADP^+$	Co^{2+}; Mg^{2+}; Mn^{2+}	Takahashi et al., 1998	EG12715
IspD/ *ispD*	2-*C*-methyl-D-erythritol-4-phosphate + CTP + H^+ / 4-(cytidine 5'-diphospho)-2-*C*-methyl-D-erythritol + diphosphate	CTP; Co^{2+}; Mg^{2+}; Mn^{2+}	Rohdich et al., 1999	G7423
IspE/ *ispE*	4-(cytidine 5'-diphospho)-2-*C*-methyl-D-erythritol + ATP / 2-phospho-4-(cytidine 5'-diphospho)-2-*C*-methyl-D-erythritol + ADP + 2 H^+	ATP;	Lüttgen et al., 2000; Lange & Croteau 1999	EG11294
IspF/ *ispF*	2-phospho-4-(cytidine 5'-diphospho)-2-*C*-methyl-D-erythritol / CMP + 2-*C*-methyl-D-erythritol-2,4-cyclodiphosphate	Mn^{2+}	Herz et al. 2000	EG11816
IspG/ *ispG* (*gcpE*)	2-*C*-methyl-D-erythritol-2,4-cyclodiphosphate + [reduced ferredoxin]$_2$ / 1-hydroxy-2-methyl-2-(E)-butenyl 4-diphosphate + [oxidized ferredoxin]$_2$ + H_2O	Mn^{2+}; flavodoxin or ferredoxin; NAD(P)H; [4Fe-4S] cluster	Altincicek et al., 2001; Seemann et al., 2002; Zepeck et al., 2005	EG10370

IspH/ *ispH* (*lytB*)	NADPH + 1-hydroxy-2-methyl-2-(E)-butenyl 4-diphosphate + H^+/ $NAD(P)^+$ + dimethylallyl diphosphate + isopentenyl diphosphate + H_2O	Co^{2+} ; flavodoxin or ferredoxin; NAD(P)H; [4Fe-4S] cluster	Rohdich et al., 2002; Seemann and Rohmer, 2007	EG11081

Table 2: Strains and plasmids acquired for this study.

Strain	Genotype	Source
Saccharomyces cerevisiae		
F1702	*MAT***a** *ade1 arg4 his2 leu2 trp1 ura3*	Dr. G. Fink, Whitehead Institute, Cambridge, MA
CEN.PK 113-7D	*MATα MAL2-8^c SUC2*	Dr. P. Kötter, Frankfurt, Germany.
JAY20	*MATα leu1 ura3-52* (derived from FY2, Winston et al. 1995)	Dr. J. Avalos and Dr. G. Fink, Whitehead Institute, Cambridge, MA
Escherichia coli		
MAX Efficiency® DH5α™	F$^-$ φ80*lacZΔM15* Δ(*lacZYA-argF*) U169 *recA1 endA1 hsdR17* (rk-, mk+) *phoA supE44* λ$^-$ *thi-1 gyrA96 relA1*	Life Technologies, Grand Island, NY
K-12, MG1655	F$^-$ lambda$^-$ *ilvG rfb-50 rph-1*	Ajikumar et al., 2010

Plasmid name	Origin/reference
pKT127	Sheff and Thorn, 2004.
pRS414TEF	Mumberg et al., 1995
pRS415GPD	Mumberg et al., 1995
PUCAR1	Dr. Hang Zhou
pUC19	Life Technologies, Grand Island, NY
PUG72	Güldener et. al., 2002
pESC-URA	Stratagene, Agilent Technologies, Inc., Santa Clara, CA

Table 3: Primers.

Feature	Forward[1] primer (5' - 3')	Reverse[1] Primer (5' - 3')	Amplicon size (bp)[2]	Restriction sites[3]
yeGFP	GACTTAACTAGTATGT CTAAAGGTGAAGAATT ATTCACTGG	TATGACCTCGAGTT ATTTGTACAATTCAT CCATACCATGGG	717	*Spe*I/*Xho*I
ADH1t	GACTTACTCGAGGCGA ATTTCTTATGATTTAT GATTTTTATTATTAAA TAAGT	TATGACGGTACCGA GCGACCTCATGCTA TACCTG	166	*Xho*I/*Kpn*I
PGK1p	GACTTAGAGCTCAGAC GCGAATTTTTCGAAGA AGTACC	TATGACACTAGTTG TTTTATATTTGTTGT AAAAAGTAGATAAT TACTTCC	1000	*Sac*I/*Spe*I
ACT1t	GACTTACTCGAGTCTC TGCTTTTGTGCGCGTA TGT	TATGACGGTACCAT ATGATACACGGTCC AATGGATAAAC	293	*Xho*I/*Kpn*I
TEF2p	GACTTAGAGCTCGGGC GCCATAACCAAGGTAT C	TATGACACTAGTGT TTAGTTAATTATAGT TCGTTGACCGTATA	500	*Sac*I/*Spe*I
ENO2t	GACTTACTCGAGAGTG CTTTTAACTAAGAATT ATTAGTCTTTTCTG	TATGACGGTACCAG GTATCATCTCCATCT CCCATATG	400	*Xho*I/*Kpn*I
HIS2	GACTTAAAGCTTTCAA TCTTGCCGGTTTCATA CATGTTG	TATGACAAGCTTAA AGGTTTCCCAGCCA AACCCG	1750	*Hin*dIII
ADE1	GACTTAAAGCTTATTC ACGAGTCAGTCTGACT CTTG	TATGACAAGCTTGA ATACGAAAGAGAAC TGAGTCAGTTG	1427	*Hin*dIII
YPRCδ15-	GACTTAGACGTCTTAA TTAAGCCAGGCGCCTT	TATGACGTCGACGC GGCCGCTGACCTAG	690	*Aat*II-*Pac*I/*Sal*I-

UP	TATATCAT	ACCTAGGTTTGCGAAACCCTATGCTCT		*Not*I-*Avr*II
YPRCδ15-DOWN	GACTTAGCTAGCAATGGAAGGTCGGGATGAG	TATGACGCGGCCGCTGACCTAGACCTAGGATAAAGCAGCCGCTACCAAA	651	*Nhe*I/*Not*I-*Avr*II
YPRCτ3-UP	GACTTAGACGTCTTAATTAAAAAGGAGGTGCACGCATTAT	TATGACGTCGACGCGGCCGCTGACCTAGACCTAGGTTCCAAGGAGGTGAAGAACG	598	*Aat*II-*Pac*I/*Sal*I-*Not*I-*Avr*II
YPRCτ3-DOWN	GACTTAGCTAGCGATGGGACGTCAGCACTGTA	TATGACGCGGCCGCTGACCTAGACCTAGGCGGTATTACTCGAGCCCGTA	638	*Nhe*I/*Not*I-*Avr*II
Expression cassettes	GACTTAGCTAGCCCTCACTAAAGGGAACAAAAGCTG	TATGACGCGGCCGCTGACCTAGACCTAGGAATACGACTCACTATAGGGCGAATTG	Variable	*Nhe*I/*Not*I-*Avr*II
TRP1	GACTTAGCTAGCGTACAATCTTGATCCGGAGCTTTTC	TATGACGCGGCCGCTGACCTAGACCTAGGAGGCAAGTGCACAAACAATACTTAAATAAATA	870	*Nhe*I/*Not*I-*Avr*II
LEU2	GACTTAGCTAGCTCGACGGTCGAGGAGAACTTC	TATGACGCGGCCGCTGACCTAGACCTAGGTCGACTACGTCGTAAGGCCG	2235	*Nhe*I/*Not*I-*Avr*II
ERG13-UP	CGGAATAAGCTTCGTATATACAATAGAAAAATTTTC	TATGACCTGCAGGCTGCACCTTTTATAGTAATTTGGCTAC	213	*Hin*dIII/*Pst*I
ERG13-DOWN	GACTTAACTAGTCCCGGGTCTTCCCCCATCGATTGCATCTTG	TATGACCCGCGGCGGCCGGGAAAACACGTCGGGGTTATGAATG	272	*Spe*I/*Sac*II

ERG13-Delta(1)	CACTATCCATCCGACAGATGGAC	ACCAAGGGGATTATTGATGCTTGCT	1000	
ERG13-Delta(2)	TTGAGATGAGCTTAATCATGTCAAAGC	GATGTTTCTAAAGTGGCCTGTACG	900	
ERG13	ATGAAACTCTCAACTAAACTTTGTTGGTG	TTTTTTAACATCGTAAGATCTTCTAAATTTGTCATC	1473	
leuC	GACTTAGGATCCATGGCTAAGACGTTATACGAAAAATTGTTC	TATGACAAGCTTTTATTTAATGTTGCGAATGTCGGCGAAATG	1401	*Bam*HI/*Hin*dIII
leuD	GACTTAGAATTCATGGCAGAGAAATTTATCAAACACACAG	TATGACGAGCTCTTAATTCATAAACGCAGGTTGTTTTGCTTC	606	*Eco*RI/*Sac*I
LEU1	GACTTAGGATCCATGGTTTACACTCCATCCAAGGG	TATGACCTCGAGCTACCAATCCTGGTGGACTTTATC	2340	*Bam*HI/*Xho*I
TEF1p-dxs-ADH1t	CGAGGGGCCCGCTGGAGCTCATAGCTTC	CCAGCGACGTCTACCGAGCGACCTC	2483	*Apa*I/*Aat*II
PGK1p-ispF-ACT1t	CCCAGCATGCAGACGCGAATTTTTCG	CTAGACCTAGGGCGAATTGGGTACCGGCCGC	1806	*Sph*I/*Afl*II
TDH3p-ispE-CYC1t	CGGTAGACGTCGCTGGAGCTCAGTTTATC	CTAGACCTAGGGCGAATTGGGTACCGG	1823	*Aat*II/*Avr*II
TEF1p-ispD-CYC1t	GCTAGGCGCCGGGAACAAAAGCTGGAGCTCATAGC	GTACCATATGCGACTCACTATAGGGCGAATTGGG	1450	*Kas*I/*Nde*I
TEF1p-ispG-CYC1t	CTGCAGGCATGCAAGCTTGAATACGAAAGAG	GACCGTGTATCATATCGGCCGGTACCCACTTAAGGGC	1879	*Sph*I/*Afl*II
TDH3p-ispH-CYC1t	GGTAGACGTCGCTGGAGCTCAGTTTATCATTATC	GCTCCTAGGGCGAATTGGGTACCGGCCGC	1919	*Aat*II/*Avr*II

PGK1p-ispC-ACT1t	CGCCCTAGGAGCTGGAGCTCAGACGCGAATTTTTC	GCCCTTAAGTGGGTACCGGCCGATATGATACAC	2544	*Avr*II/*Afl*II
TEF1p-idi-ADH1t	GAGGGGCCCGCTGGAGCTCATAGCTTC	CAGCGACGTCTACCGAGCGACCTCATGC	1167	*Apa*I/*Aat*II
TDH3p-YtfE-CYC1t	CTAGAGGATCCCCGGGTACCGCTGGAGCTCAGTTTATCATTATC	CACTTAAGGGCCGCAAATTAAAGCCTTCGAGCGTCCC	1626	*Bam*HI/*Afl*II
TEF1p-bfr-ADH1t	CGAGGGGCCCGCTGGAGCTCATAGCTTC	CCAGCGACGTCTACCGAGCGACCTCATGCTATAC	1511	*Apa*I/*Aat*II
PGK1p-bfd-ACT1t	CGCCCTAGGAGCTGGAGCTCAGACGCGA	GGCCCTTAAGTGGGTACCGGCCGATATGATACACGGTCCAATG	1546	*Avr*II/*Afl*II
TDH3p-FtnA-CYC1t	CGGTAGACGTCGCTGGAGCTCAGTTTATCATTATC	GCTCCTAGGGCGAATTGGGTACCCGGCCGCAAATTAAAGCCTTCG	1468	*Aat*II/*Avr*II
ARG4	CGCCAAGCTTCACTGTCAGAGACTGTTTCC	GAGGATCCAGAGTCGACAACGACTTTGGGAGG	2320	*Hin*dIII/*Bam*HI

[1] Primer direction defined according to the direction of translation of the ORF.

[2] Amplicon size does not include adaptamers containing the restriction sites.

[3] Restriction site(s) in the adaptamer of the forward primer / restriction site(s) in the adaptamer of the reverse primer.

Table 4: ORFs and primers.

ORF name	Forward[1] primer (5' - 3')	Reverse[1] Primer (5' - 3')	EcoCyc accession number	Expression cassette
dxs[2]	ATGTCATTTGATATTG CCAAGTACCC	CTATGCCAACCAAGCC TTAATTTTC	G6237	TEF1p/ADH1t
dxr[2]	ATGAAACAATTAACG ATTCTTGGCTCAAC	TCAGGATGCTAACCTC ATTACTTCTTT	EG12715	PGK1p/ACT1t
ispD[2]	ATGGCAACAACGCACT TGGATG	TTACGTGTTTTCTTGGT GAATTGTTCTTG	G7423	TEF1p/ADH1t
ispE[2]	ATGAGAACTCAGTGGC CTAGTC	TTAAAGCATGGCTCTAT GAAGTGGG	EG11294	TDH3p/CYC1t
ispF[2]	ATGAGAATTGGTCACG GCTTCG	CTATTTCGTTGCCTTGA TCAACAAG	EG11816	PGK1p/ACT1t
ispG[2]	ATGCATAACCAAGCAC CCATCC	TCATTTTTCAACTTGCT GTACATCTATCC	EG10370	TEF1p/ADH1t
ispH[2]	ATGCAAATATTGTTGG CTAATCCCAG	TCAGTCGACTTCTCTAA TATCAACAC	EG11081	TDH3p/CYC1t
idi[2]	ATGCAAACTGAGCAC GTAATTCTG	CTACTTTAACTGGGTGA ATGCAGAT	G7508	TEF1p/ADH1t
iscX	GACTTAACTAGTATGG GACTTAAGTGGACCGA TAG	TATGACCTCGAGTTATT CGGCCTCGTCCAGCC	EG12311	TEF2p/ENO2t
iscR	GACTTAACTAGTATGA GACTGACATCTAAAGG GCG	TATGACCTCGAGTTATT AAGCGCGTAACTTAAC GTCGATC	G7326	TEF1p/ADH1t
iscS	GACTTAACTAGTATGA AATTACCGATTTATCT	TATGACCTCGAGTTAAT GATGAGCCCATTCGAT	G7325	PGK1p/ACT1t

	CGACTACTC	GCTG		
iscA	GACTTAACTAGTATGT CGATTACACTGAGCGA CAGT	TATGACCTCGAGTCAA ACGTGGAAGCTTTCGC CG	EG12132	PGK1p/ACT1t
iscU	GACTTAACTAGTATGG CTTACAGCGAAAAAGT TATCGAC	TATGACCTCGAGTTATT TTGCTTCACGTTTGCTT TTATAGTCC	G7324	PGK1p/ACT1t
HscA	GACTTAACTAGTATGG CCTTATTACAAATTAG TGAACCTG	TATGACCTCGAGTTAA ACCTCGTCCACGGAAT GGC	EG12130	TEF1p/ADH1t
HscB	GACTTAACTAGTATGG ATTACTTCACCCTCTTT GGC	TATGACCTCGAGTTAA AAATCGAGCAGTTTTTC TTCGAGTTG	EG12131	TEF1p/ADH1t
CyaY	GACTTAACTAGTATGA ACGACAGTGAATTTCA TCGCC	TATGACCTCGAGTTAG CGGAAACTGACTGTTT CACC	EG11653	TEF2p/ENO2t
ErpA	GACTTAACTAGTATGA GTGATGACGTAGCACT GC	TATGACCTCGAGTTAG ATACTAAAGGAAGAAC CGCAAC	EG12332	TEF2p/ENO2t
bfr	GACTTAACTAGTATGA AAGGTGATACTAAAGT TATAAATTATCTCAAC	TATGACCTCGAGTCAA CCTTCTTCGCGGATCTG TG	EG10113	TEF1p/ADH1t
FtnA	GACTTAACTAGTATGC TGAAACCAGAAATGA TTGAAAAACTTAAT	TATGACCTCGAGTTAGT TTTGTGTGTCGAGGGTA GAG	EG10921	TDH3p/CYC1t
bfd	GACTTAACTAGTATGT ACGTTTGTCTTTGTAA TGGTATCAG	TATGACCTCGAGTTATG CGGACTCCTTAAACTCC G	EG11181	PGK1p/ACT1t
fdx	GACTTAACTAGTATGC CAAAGATTGTTATTTT GCCTCATC	TATGACCTCGAGTTAAT GCTCACGCGCATGGTT GAT	EG11328	TDH3p/CYC1t
fpr	GACTTAACTAGTATGG CTGATTGGGTAACAGG	TATGACCTCGAGTTACC AGTAATGCTCCGCTGTC	EG10628	TDH3p/CYC1t

	CAAA	ATA		
FldA	GACTTAACTAGTATGG CTATCACTGGCATCTT TTTCG	TATGACCTCGAGTCAG GCATTGAGAATTTCGTC GAGA	EG10318	TDH3p/CYC1t
YtfE	GACTTAACTAGTATGG CTTATCGCGACCAACC TTTA	TATGACCTCGAGTCACT CACCCGCCAGCGCGC	G7866	TDH3p/CYC1t

[1] Primer direction defined according to the direction of translation of the ORF.

[2] These genes were purchased codon optimized with flanking restriction sites and sub-cloned so no primers were required to clone these genes into their individual expression cassettes. The primers listed here are therefore the primers used for verification of genomic inserts and RT-PCR.

Table 5: Plasmids constructed in this study.

Plasmid name	Origin	Auxotrophic marker	Description
pSCX001	pRS414TEF	*TRP1*	Plasmid for test of expression cassette with GFP
pSCX002	pRS414TEF	*TRP1*	Plasmid for test of expression cassette with GFP
pSCX003	pRS415GPD	*LEU2*	Plasmid for test of expression cassette with GFP
pSCX004	pRS414TEF	*TRP1*	Plasmid for test of expression cassette with GFP
pSC604	pUC19	*HIS2*	Plasmid for genomic integration of *dxs*, *ispD*, *ispE* and *ispF* expression cassettes
pSC704	pUC19	*ADE1*	Plasmid for genomic integration of *dxr*, *ispG*, *ispH* and *idi* expression cassettes
pSC804	pUCAR1	*ARG4*	Plasmid for genomic integration of *bfr*, *FtnA*, *bfd* and *YtfE* expression cassettes
pSCFeS107TRP	pUC19	*TRP1*	Plasmid for genomic integration of *iscX*, *iscR*, *iscS*, *fdx*, *CyaY* and *iscU* expression cassettes
pSCFeS207LEU	pUC19	*LEU2*	Plasmid for genomic integration of *HscB*, *fpr*, *iscA*, *ErpA*, *HscA* and *FldA* expression cassettes
pSCΔ001	pUG72	*URA3*	Plasmid for deletion of ERG13
pESC-leuC	pESC-URA	*URA3*	2µ plasmid for expression of *leuC*
pESC-leuC-D	pESC-leuC	*URA3*	2µ plasmid for expression of *leuC* and *leuD*
pESC-LEU1	pESC-LEU1	*URA3*	2µ plasmid for expression of *leu1*

Table 6: *S. cerevisiae* strains constructed in this study

Strain	Parental strain	Auxotrophic markers	Integrated plasmid or cassette	Integration locus or *S. cerevisiae* origin of replication
SCX001	F1702	*ade1 arg4 his2 leu2 ura3*	pSCX001	CEN6-ARSH4
SCX002	F1702	*ade1 arg4 his2 leu2 ura3*	pSCX002	CEN6-ARSH4
SCX003	F1702	*ade1 arg4 his2 trp1 ura3*	pSCX003	CEN6-ARSH4
SCX004	F1702	*ade1 arg4 his2 leu2 ura3*	pSCX004	CEN6-ARSH4
SC704	F1702	*arg4 his2 leu2 trp1 ura3*	pSC704	YAR015W
SCMEP	SC704	*arg4 leu2 trp1 ura3*	pSC604	YFR025C
SCMEP-FeS1	SCMEP	*arg4 trp1 ura3*	pSCFeS207LEU	YPRCτ3
SCMEP-FeS2	SCMEP-FeS1	*arg4 ura3*	pSCFeS107TRP	YPRCδ15
SCMEP-FeS2-IS	SCMEP-FeS2	*ura3*	pSC804	YHR018C
SCMEP-FeS2-IS-ΔERG13	SCMEP-FeS2-IS	Prototrophic	pSCΔ001	YML126C
SC-pESC	JAY20	*leu1*	pESC-URA	2μ
SC-leuC	JAY20	*leu1*	pESC-leuC	2μ
SC-leuC-D	JAY20	Prototrophic	pESC-leuC-D	2μ
SC-LEU1	JAY20	Prototrophic	pESC-LEU1	2μ

Figure Captions

Figure 1: **Overview of isoprenoids biosynthetic pathways.** Green gene names are mevalonate pathway genes and red gene names are 2-*C*-methyl-D-erythritol-4-phosphate (MEP) pathway genes. Gene / protein: *ERG10* / acetoacetyl-CoA thiolase, *ERG13* / 3-hydroxy-3-methyl-glutaryl-CoA synthase, *HMG1* and *HMG2* / 3-hydroxy-3-methyl-glutaryl-CoA reductase, *ERG12* / mevalonate kinase, *ERG8* / phosphomevalonate kinase, *ERG19* / mevalonate-5-diphosphate decarboxylase, *IDI* and *idi* / isopentenyl diphosphate isomerase, *ERG20* / Farnesyl diphosphate synthase, *dxs* / 1-deoxy-D-xylulose-5-phosphate synthase, *dxr* / 1-deoxy-D-xylulose-5-phosphate reductase, *ispD* / 4-diphosphocytidyl-2-*C*-methyl-D-erythritol synthase, *ispE* / 4-diphosphocytidyl-2-*C*-methyl-D-erythritol kinase, *ispF* / 2-*C*-methyl-D-erythritol 2,4-cyclodiphosphate synthase, *ispG* / 1-hydroxy-2-methyl-2-(E)-butenyl-4-phosphate synthase, *ispH* / 1-hydroxy-2-methyl-2-(E)-butenyl-4-phosphate reductase. Pathway intermediates: FBP – fructose bisphosphate, DHAP - dihydroxyacetone phosphate, G3P – glyceraldehyde 3-phosphate, PEP – phosphoenolpyruvate, PYR – pyruvate, ACCoA – acetyl-CoA, AcACCoA – acetoacetyl-CoA, HMG-CoA – 3-hydroxy-3-methyl-glutaryl-CoA, MEV – mevalonate, MEV-P – mevalonate-5-phosphate, MEV-PP – mevalonate diphosphate, IPP – isopentenyl diphosphate, DMAPP – dimethylallyl diphosphate, FPP – farnesyl diphosphate, DXP – 1-deoxy-D-xylulose-5-phosphate, MEP – 2-*C*-methyl-D-erythritol-4-phosphate, CDP-ME – 4-diphosphocytidyl-2-*C*-methyl-D-erythritol, CDP-MEP – 2-phospho-4-diphosphocytidyl-2-*C*-methyl-D-erythritol, MEC – 2-*C*-methyl-D-erythritol-2,4-cyclodiphosphate, HMBP – 1-hydroxy-2-methyl-2-(E)-butenyl-4-phosphate.

Figure 2. **Verification of genomic integrated genes in SCMEP-FeS2-IS strain and deletion of *ERG13*.** (A) To verify that all the genes had been inserted into the genome of SCMEP-FeS2-IS, gDNA was purified and used as template for amplification of the individual ORFs using primer pairs listed in Table 4. The amplification product was visualized by gel-electrophoresis on 0.75% agarose gel in TAE–buffer. Numbering of lanes corresponds to the following ORFs: 1: *iscX* (0.20 kb), 2: *iscR* (0.49 kb), 3: *iscS* (1.22 kb), 4: *fdx* (0.34 kb), 5: *CyaY* (0.32 kb), 6: *iscU* (0.39 kb), 7: *hscB* (0.52 kb), 8: *fpr* (0.75 kb), 9: *iscA* (0.32 kb), 10: *erpA* (0.35 kb), 11: *hscA* (1.85 kb), 12: *fldA* (0.53 kb), 13: *bfr* (0.48 kb), 14: *FtnA* (0.50 kb), 15: *bfd* (0.20 kb), 16: *YtfE* (0.66 kb), *17: dxs* (1.86 kb), 18: *ispE* (0.85 kb), 19: *ispF* (0.48 kb), 20: *ispD* (0.71 kb), 21: *idi*

(0.55 kb), 22: *ispH* (0.95 kb), 23: *dxr* (1.19 kb), 24: *ispG* (1.12 kb). **(B)** gDNA purified from the following strains; 1: SCMEP-FeS2-IS-ΔERG13-colony13, 2: SCMEP-FeS2-IS-ΔERG13-colony25, 3: SCMEP-FeS2-IS-ΔERG13-colony29 and 4: F1702 was used as templates for PCR reactions using the primers shown in Table 3. The PCR reactions of the ERG13UP (1.00 kb) and ERG13DOWN (0.90 kb) fragments verify that the deletion cassette has been inserted in the correct locus, and the inability to amplify the ERG13ORF (1.47 kb) from templates 1, 2 and 3 verifies that *ERG13* has not been duplicated prior to the knockout.

Figure 3. Ergosterol Mass isotopomer distribution. Integration of the peak areas of the ergosterol 468 Dalton (corresponding to M0) and 27 of its mass isotopomers (only the first 8 are shown since the area of every mass isotopomer peak above 5 is close to 0) at increments of 1 Dalton normalized to the total abundance. The labeled results are from ergosterol extracted from SCMEP-FeS-IS-ΔERG13 grown on U-$13C_6$ glucose whereas the unlabeled results are from SCMEP-FeS-IS-ΔERG13 grown on regular glucose. The experiment was done in biological triplicates.

Figure 4. Verification of gene expression by Reverse Transcription PCR. To find out if the genes inserted in the genome of SCMEP-FeS2-IS are transcribed, total RNA was purified and used as template for amplification of the individual ORFs by RT-PCR using the primer pairs listed in Table 4. The amplification product was visualized by gel electrophoresis on 0.75% agarose gel in TAE–buffer. Numbering of lanes corresponds to the following ORFs: 1: *iscX* (0.20 kb), 2: *iscR* (0.49 kb), 3: *iscS* (1.22 kb), 4: *fdx* (0.34 kb), 5: *CyaY* (0.32 kb), 6: *iscU* (0.39 kb), 7: *hscB* (0.52 kb), 8: *fpr* (0.75 kb), 9: *iscA* (0.32 kb), 10: *erpA* (0.35 kb), 11: *hscA* (1.85 kb), 12: *fldA* (0.53 kb), 13: *bfr* (0.48 kb), 14: *FtnA* (0.50 kb), 15: *bfd* (0.20 kb), 16: *YtfE* (0.66 kb), *17: dxs* (1.86 kb), 18: *ispE* (0.85 kb), 19: *ispF* (0.48 kb), 20: *ispD* (0.71 kb), 21: *idi* (0.55 kb), 22: *ispH* (0.95 kb), 23: *dxr* (1.19 kb), 24: *ispG* (1.12 kb).

Figure 5. OD_{600} measured during serial sub-culturing. Three strains of SCMEP-FeS-IS-ΔERG13 were grown on SC-ADE-ARG-HIS-LEU-TRP-URA supplemented with mevalonolactone. The cultures were inoculated at OD_{600} = 0.1 at each sub-culturing and the mevalonolactone concentration gradually reduced. The OD_{600} was measured after each sub-culturing which lasted for 5 days

Figure 6. Microscope pictures of evolved SCMEP-FeS-IS-ΔERG13 strains. The strains were grown in SC-ADE-ARG-HIS-LEU-TRP-URA + 0.25 g/l mevalonolactone for 5 days before the morphology was assessed by light-microscopy. A: SCMEP-FeS-IS-ΔERG13-strain13, B: SCMEP-FeS-IS-ΔERG13-strain25, and C: SCMEP-FeS-IS-ΔERG13-strain29.

Figure 7. Complementation of the *leu1* auxotrophy in the JAY20 *S. cerevisiae* strain. JAY20 transformed with pESC-URA, pESC-leuC-D, pESC-LEU1 and pESC-leuC was plated on SC-LEU-URA and incubated at 30 °C for 3 days.

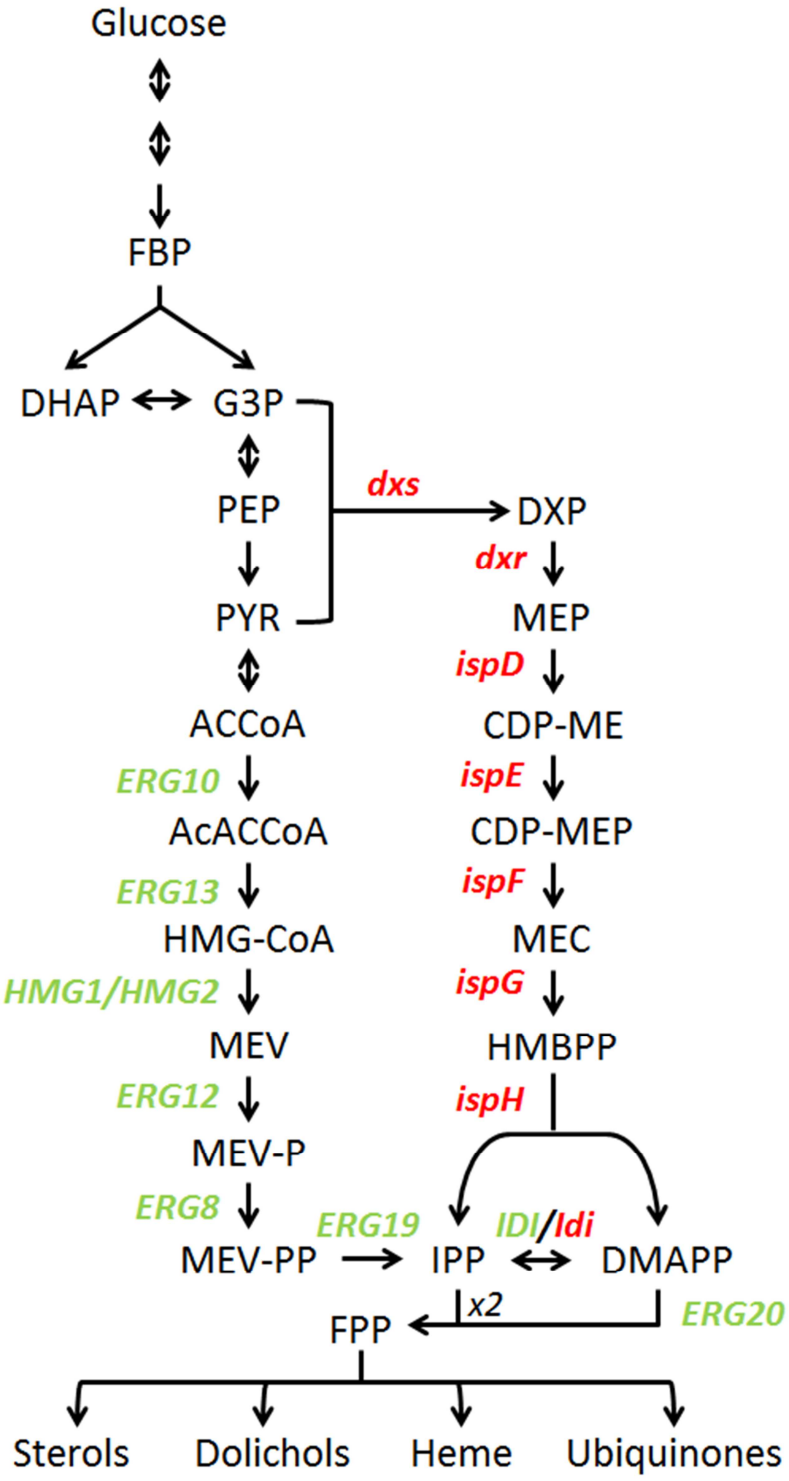
Glucose
FBP
DHAP
G3P
PEP
PYR
dxs
DXP
dxr
MEP
ispD
CDP-ME
ACCoA
ERG10
ispE
CDP-MEP
AcACCoA
ERG13
ispF
MEC
HMG-CoA
HMG1/HMG2
ispG
HMBPP
MEV
ERG12
ispH
MEV-P
ERG8
ERG19
IDI/Idi
MEV-PP
IPP
DMAPP
x2
ERG20
FPP
Sterols
Dolichols
Heme
Ubiquinones

Figure 1


A
pSCFeS107TRP
1 2 3 4 5 6
pSCFeS207LEU
7 8 9 10 11 12
pSC804
13 14 15 16
pSC604 + pSC704
17 18 19 20 21 22 23 24
B
ERG13UP
1 2 3 4
ERG13DOWN
1 2 3 4
ERG13ORF
1 2 3 4

Figure 2

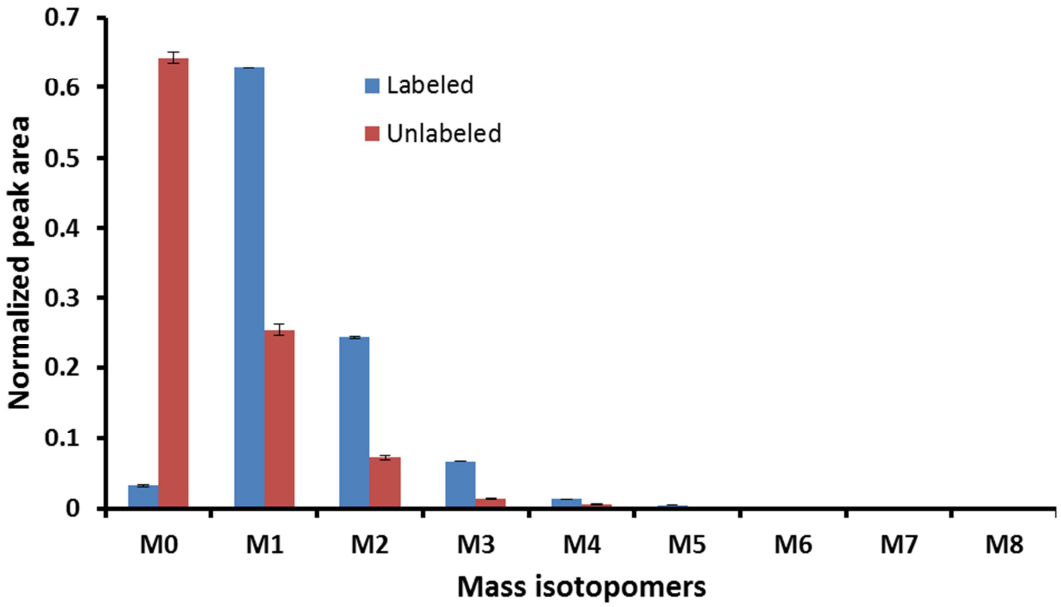
0.7
0.6
0.5
0.4
0.3
0.2
0.1
0
Normalized peak area
Labeled
Unlabeled
M0
M1
M2
M3
M4
M5
M6
M7
M8
Mass isotopomers

Figure 3

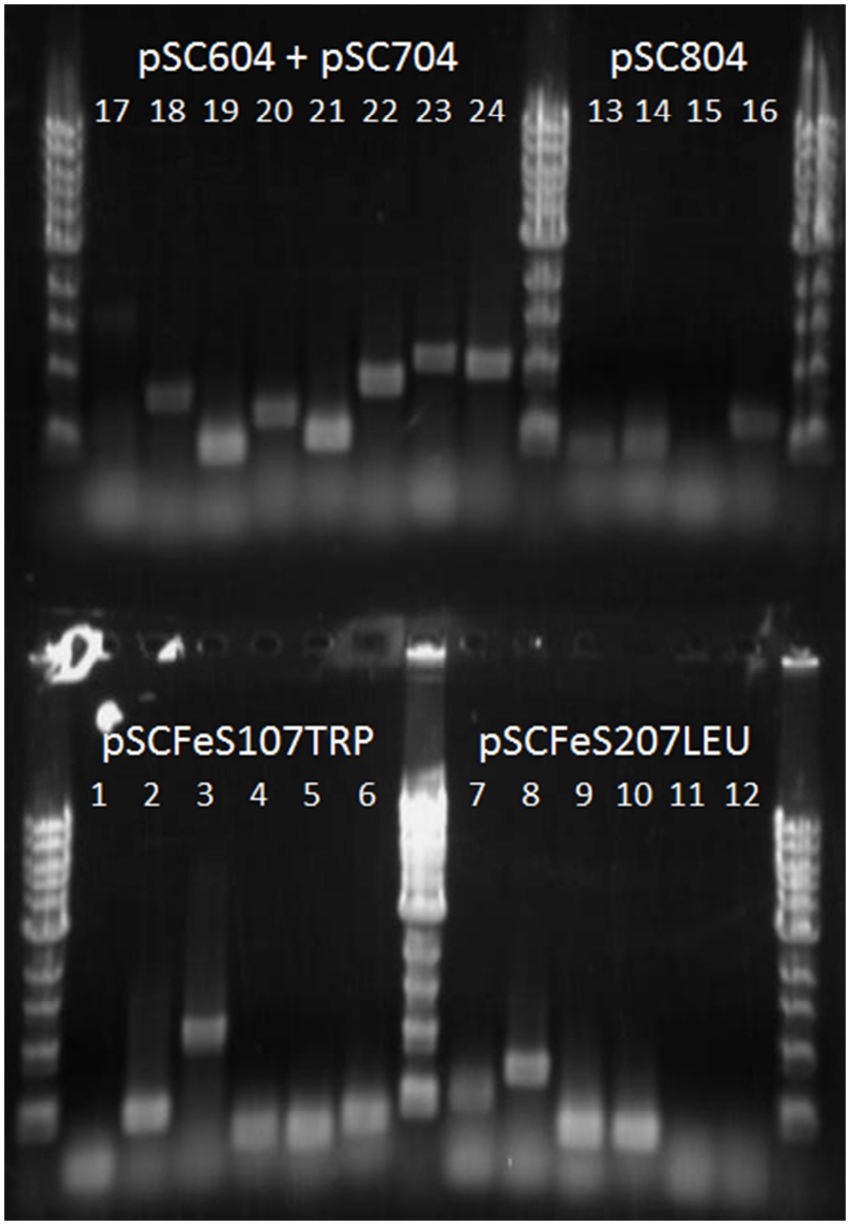
pSC604 + pSC704
17 18 19 20 21 22 23 24
pSC804
13 14 15 16
pSCFeS107TRP
1 2 3 4 5 6
pSCFeS207LEU
7 8 9 10 11 12

Figure 4

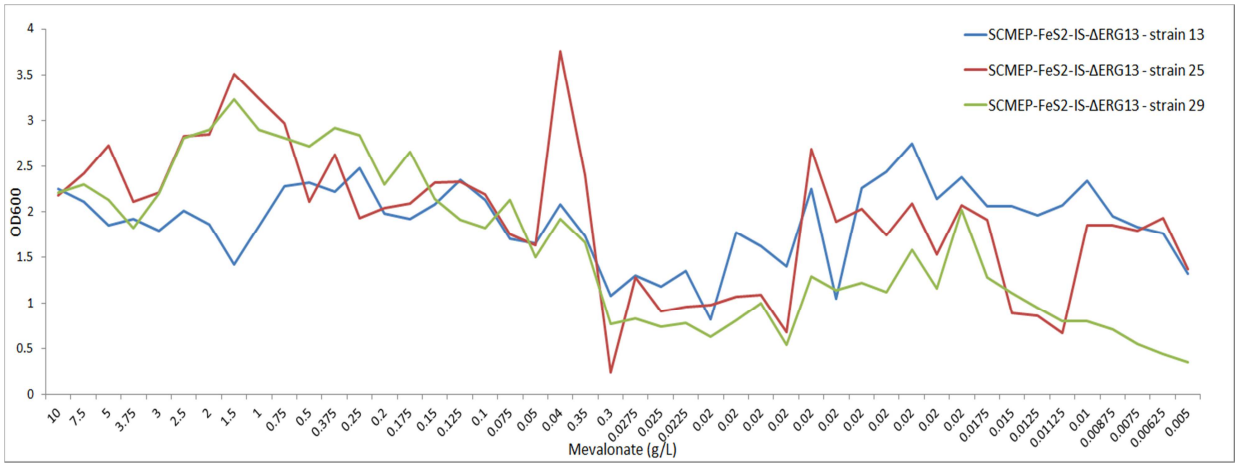
SCMEP-FeS2-IS-ΔERG13 - strain 13
SCMEP-FeS2-IS-ΔERG13 - strain 25
SCMEP-FeS2-IS-ΔERG13 - strain 29
OD600
Mevalonate (g/L)

Figure 5

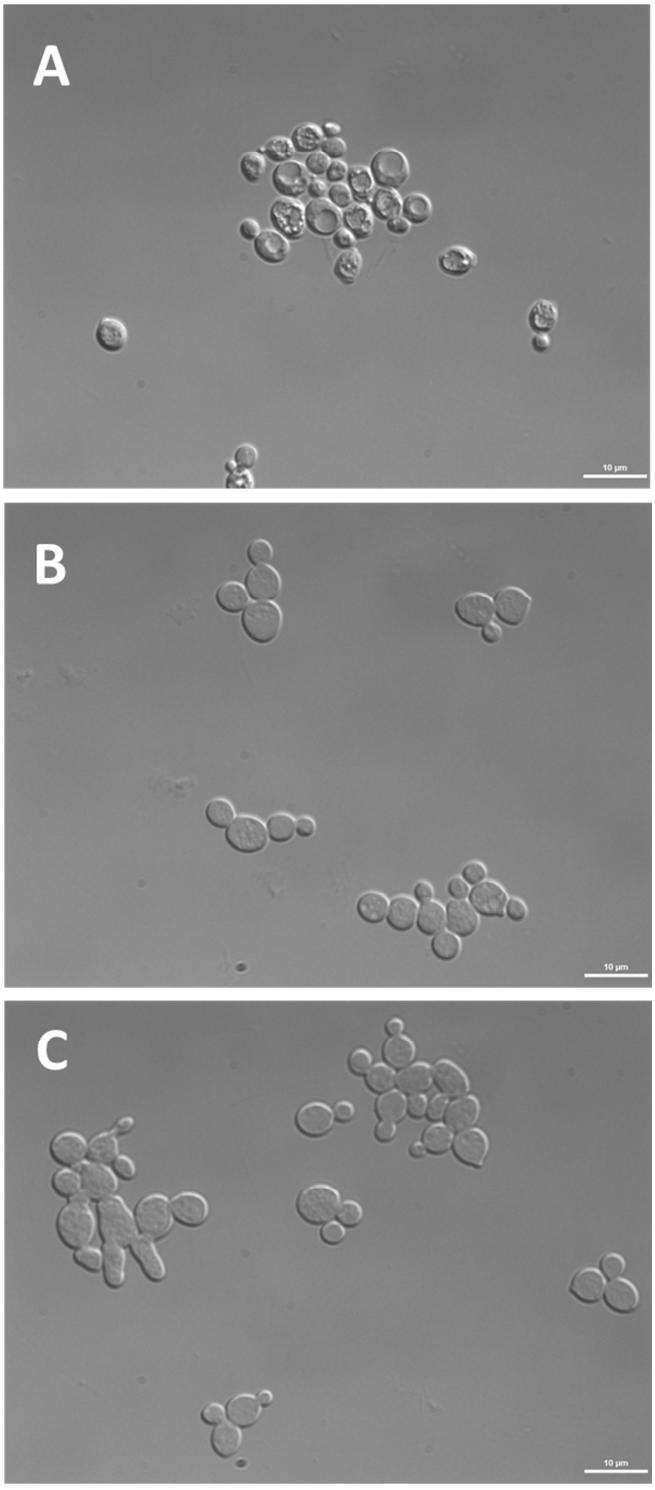

Figure 6

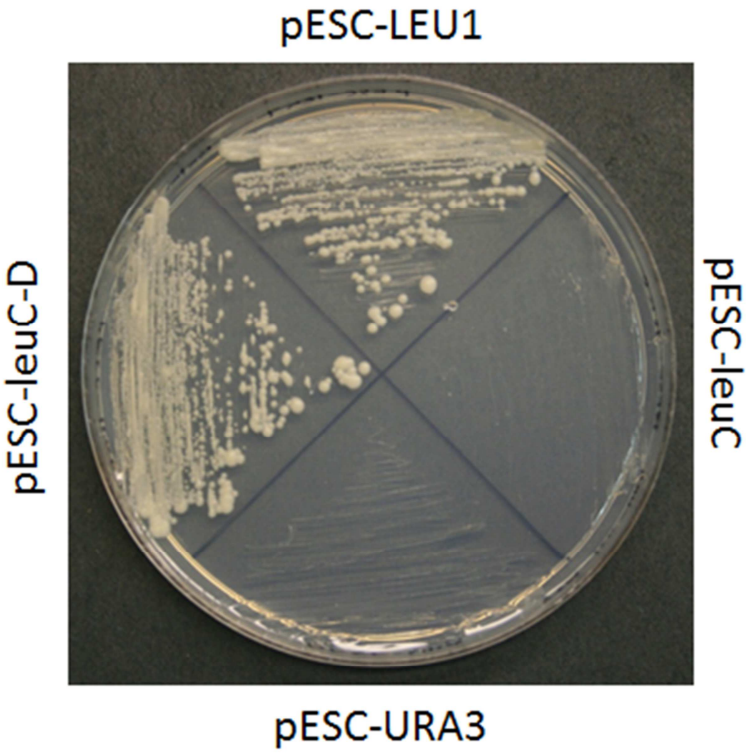

Figure 7